Chapter 10
Advances in Modeling of Water Quality in Estuaries

Isabella Ascione Kenov, Francisco Campuzano, Guilherme Franz, Rodrigo Fernandes, Claudia Viegas, João Sobrinho, Hilda de Pablo, Andreia Amaral, Ligia Pinto, Marcos Mateus, and Ramiro Neves

Abstract Water quality models are in great demand to complement studies about the status of estuarine waters. However, local models do not perform well when boundary conditions are not properly defined and when biogeochemical processes are not described with adequate detail. This chapter presents advanced modeling applications to perform water quality studies in Portuguese estuaries. Boundary conditions for hydrodynamics and biogeochemistry are provided by the Portuguese Coast Operational Model, downscaled by using nested domains with increasing resolution from the regional to the local scale. The nested models of the estuaries are described, and case studies are presented for specific estuaries to compute sediment transport (Tagus estuary), to calculate residence time of water (Mondego estuary), to forecast quality of bathing waters (Estoril Coast), and to quantify nutrient fluxes between estuaries and the open ocean (Ria de Aveiro). The level of detail used to represent biological processes in water quality models is also addressed, including the description of a case study about modeling of species vulnerable to water quality, such as *Zostera noltii* in Ria de Aveiro. The need for high level of detail to represent microbial loop and carbon cycle in estuaries is discussed with the application of a complex biological model to the Tagus estuary.

10.1 Introduction

Estuaries are among the most productive environments on earth; they are considered coastal marine areas because they share more features with marine systems than with freshwater environments. Estuaries are the land-ocean link, transition

I. Ascione Kenov (✉) • F. Campuzano • G. Franz • R. Fernandes • C. Viegas • J. Sobrinho • H. de Pablo • A. Amaral • L. Pinto • M. Mateus • R. Neves
Marine Environment Technology Center (MARETEC), Instituto Superior Técnico, Universidade de Lisboa, Av. Rovisco Pais 1, 1049-001 Lisbon, Portugal
e-mail: isabella.ascione@tecnico.ulisboa.pt

C.W. Finkl and C. Makowski (eds.), *Remote Sensing and Modeling: Advances in Coastal and Marine Resources*, Coastal Research Library 9,
DOI 10.1007/978-3-319-06326-3_10,

areas between striking different environments such as land and sea, but also between fresh and seawater. Estuaries are highly dynamic in nature, with significant spatial and temporal variation on their physical and biogeochemical processes, and strong gradients in water properties. Estuaries have productive habitats with high ecological and economic importance.

Many of the world's largest cities are in coastal zones and more than 75 % of people are expected to live within 100 km of a coast by 2025 (Bulleri and Chapman 2010). Most estuaries are characterized by proximity with large cities, and receive anthropogenic inputs coming from agriculture and urban wastes with consequences on water quality. Estuarine waters are used for aquaculture farming, fishing, recreation, and navigation. The European Union (EU) lays down rules for monitoring, assessment, and management of the quality of waters, and commits EU member states to achieve good qualitative and quantitative status of all water bodies by 2015 (2000/60/EC). Huge investments have been done by EU member states to monitor, assess, and improve status of water quality of the coastal zone, including estuaries.

The assessment of the water quality is done by using both monitoring and modeling tools. In the last decades there has been a growing demand for modeling tools to support water quality management in estuarine areas. Water quality models are effective tools to simulate and predict transport of organic and inorganic substances, contaminants, and pollutants. Model results could contribute to monitoring cost savings in areas which are inaccessible to conduct sampling campaigns and experiments. Furthermore, water quality models could be used to simulate and then to evaluate different pollution and contamination scenarios, which are used for environmental impact assessment. Modeling tools are available for the modeling of rivers (Viero et al. 2013; Chibole 2013; Lai et al. 2013), lakes (Ali et al. 2013), reservoirs (Deus et al. 2013), coastal areas (Viegas et al. 2012), and estuaries (Trancoso et al. 2005; Sohma et al. 2008).

MOHID (acronym of MOdelo HIDrodinâmico) is a water modeling system developed at the Marine Environment Technology Center (MARETEC) at Instituto Superior Técnico (IST), which belongs to the Universidade de Lisboa (ULISBOA), Portugal. MOHID incorporates modules for modeling of hydrodynamics, sediment transport, and water quality, with state-of-the-art process kinetics. In this chapter, an overview of recent advances in estuarine water quality modeling with MOHID is provided. The main equations and concepts of the MOHID system are described in Sect. 10.1.1. In Sect. 10.2, advanced applications with MOHID are presented, including case studies about Portuguese estuaries. Modeling of these estuaries requires the definition of boundary conditions at the interface between the estuary and the ocean. The definition of these boundary conditions is challenging because it requires the integration between the regional scale (ocean) and the local scale (estuary). The integration of different spatial scales is achieved by the Portuguese Coast Operational Model System (PCOMS), described in Sect. 10.2.1. PCOMS is a 3-D hydrodynamic-biological operational regional model of the Portuguese coast. It includes several nested models which are used to simulate hydrodynamics and water quality of estuaries, including Tagus, Mondego, and Ria de Aveiro, among others. As such, PCOMS can be considered as a global platform feeding boundary

conditions to local scale models. These local scale models are used to support water quality studies, to answer common management question, and to improve the overall understanding of physical and ecological processes. The model of the Tagus estuary, which is nested in PCOMS, and presented in Sect. 10.2.2, is used to support water quality studies related to concerns about water clarity, pollutant distribution and sediment transport. The quality of estuarine and coastal waters used for recreational purposes is addressed in Sect. 10.2.3, with the presentation of the case study of the Estoril coast, adjacent to the Tagus mouth. The model of the Mondego estuary, described in Sect. 10.2.4, is another example for a local scale model integrated in PCOMS. It was used to solve common management questions, such as residence time of water. MOHID is a flexible tool, which can be integrated with watershed models, used to calculate freshwater inflows and nutrient inputs to estuarine systems. This multi-model integration enables the construct of an integrated and comprehensive understanding of nutrient exchanges between land, estuaries and ocean. This understanding is of importance to define the trophic status of estuarine waters in the context of the European Water framework Directives (EU WFD). The case of Ria de Aveiro, described in Sect. 10.2.5, is representative of this multi-model integration. It was applied to quantify the nutrient budget between the estuary and the ocean. Furthermore, Ria de Aveiro represents one of the most important seagrass ecosystems of Portugal. Seagrasses are very sensitive to water quality changes. For this reason, they have been recognized as important indicator species, which reflect the overall health of coastal ecosystems. Recently, a new seagrass model was developed in MOHID, to represent seagrasses in estuarine systems. The seagrass model, presented in Sect. 10.2.6, was applied to Ria de Aveiro to calculate the spatial and temporal distribution of *Zostera noltii*. Finally, the description of estuarine system often requires the use of complex models to enable a comprehensive representation of biological processes. The role of complex models for the study of estuarine processes is addressed in Sect. 10.2.7.

10.1.1 MOHID Water Modeling System

The current MOHID structure was designed in the 1990s based on the experience gained by MARETEC in the 1980s, by using the new developments of the FORTRAN 90 language, and the establishment of new standards of hierarchical data formats (HDF). To date, the developments and applications of the MOHID system include hydrodynamics (Miranda et al. 2000), wave modeling (Neves and Silva 1991), ecological modeling (Trancoso et al. 2005; Mateus et al. 2012c), Eulerian and Lagrangian transport (Pando et al. 2013; Deus et al. 2013). Presently, MOHID can handle both 2-D and 3-D simulations, Eulerian, Cartesian, and Lagrangian vertical coordinates, and a number of biogeochemical models to simulate ecological processes in water and sediment. In this section, a short description of equations and main processes simulated in MOHID is provided. Further information can be found at www.mohid.com.

10.1.1.1 Model Equations

MOHID is formulated by using the integral approach (Eq. 10.1) according to which the rate of accumulation inside a control volume equals to the sum of input and output fluxes, plus sources minus sinks:

$$\frac{\partial}{\partial t}\left(\iiint_{CV}\beta dV\right) = -\iint_{surface}\left[\left(\beta\vec{u}\cdot\vec{n}\right)+\left(-\vartheta\vec{\nabla}\ c\cdot\vec{n}\right)\right]dA+\iiint_{CV}(S_O-S_I)dV \tag{10.1}$$

where CV is the Control Volume, u is the fluid velocity relative to the surface A, ϑ is the diffusivity, β is a generic water property (such as phytoplankton, and nutrients), and S_O-S_I is the difference between sources and sinks of the property β per unit volume. By applying the Gauss's theorem to Eq. 10.1, the differential conservation equation obtained is:

$$\frac{\partial\beta}{\partial t} = -\frac{\partial}{\partial x_j}\left(u_j\beta-\vartheta\frac{\partial\beta}{\partial x_j}\right)+(S_O-S_I) \tag{10.2}$$

Following Eq. 10.2, the rate of change of a property in a point equals the divergence of the advection, plus diffusion at this point, plus the difference between production and consumption rates per unit volume. In a Lagrangian reference, the Eq. 10.2 can be rewritten as:

$$\frac{d\beta}{dt} = -\frac{\partial}{\partial x_j}\left(\vartheta\frac{\partial\beta}{\partial x_j}\right)+(S_O-S_I) \tag{10.3}$$

Following Eq. 10.3, the rate of change in a volume element equals the diffusion across its surfaces plus the difference between sources and sinks. The form of Eq. 10.3 is obtained when the surface of the control volume used in Eq. 10.1 is moving at the fluid velocity. In this case, the total volume inside the surface is constant, even if the surface is deformed. Due to random velocity associated to Brownian movement or turbulent movement, the volume will expand as a result of diffusion.

10.1.1.2 Water Processes

The conceptual diagram of MOHID water environment is described in Fig. 10.1. The water quality model used in MOHID calculates sources and sinks terms specific for each water property, in each volume element and in each time instant. The sources and sinks of a property depend on the chemical and biological processes which are involved and are associated with the biogeochemical cycles of carbon, nitrogen and phosphorus.

Air-water fluxes are computed by considering air temperature, moisture, wind speed and direction, cloud cover, precipitation, and solar radiation. At each time

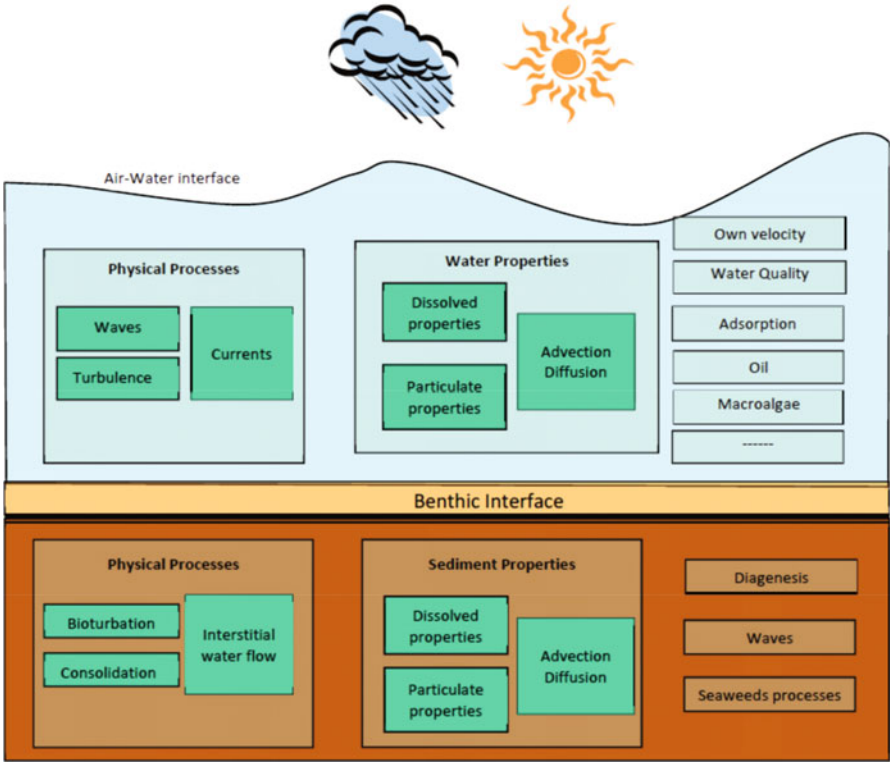

Fig. 10.1 Conceptual scheme of the MOHID aquatic environment. The water column is separated from the atmosphere by the air-water interface, and from the sediment by the benthic interface (Neves 2013)

instant the hydrodynamic model simulates the free surface elevations and velocities of the fluid necessary for calculating the terms of advection-diffusion.

The combination of transport, chemical and biological reactions in the water column, produces the spatial distribution of the water properties. MOHID offers different degrees of complexity in the description of ecological processes. According to the required level of complexity, several species of primary producers, secondary producers and decomposers in the water can be simulated. Processes at the sediment-water interface are handled in the benthic layer, where particulate matter can accumulate in a "fluff layer", and fluxes of dissolved properties are computed. Benthic organisms such as microphytobenthos, filter feeders, and deposit feeders, are assumed to be living fixed to a substrate, and interact with the environment at the water-sediment interface. Seagrasses uptake nutrients from water and sediment, while macroalgae uptake nutrients from water only, and can be transported by currents as drifting macroalgae. In the sediment, the interstitial water is transported by advection, groundwater exfiltration, and it is affected by sediment consolidation. Molecular diffusion induced by bioturbation is simulated in the upper 10 cm of sediment.

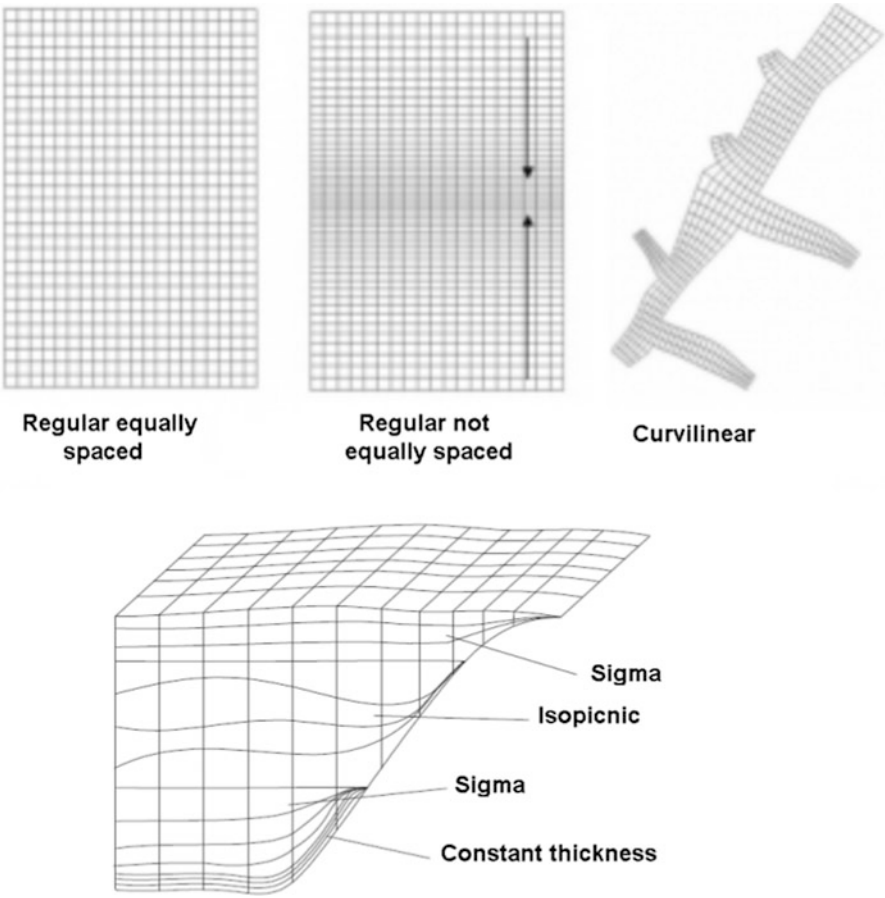

Fig. 10.2 Horizontal and vertical geometries handled by MOHID

Organic and inorganic particulate material can be transported vertically at a defined settling velocity, while oil moves vertically in the water column until it reaches a stability depth (usually the surface). Diurnal vertical migrations of fish larvae and dinoflagellates can be simulated as well.

10.1.1.3 Horizontal Geometry

Mathematical models describe nature by using discrete values computed in a grid. MOHID can handle constant spacing grids, irregular grids and curvilinear grids (Fig. 10.2). Regular equally spaced grids have squared cells, and are used to give the same importance to all the areas of the represented geographic domain. These grids can be rotated to adapt the simulated domain to the inclination of the coast. Regular not-equally spaced grids are used when some areas have to be described at

different resolution. As an example, a regular not-equally spacing grid can be used with low resolution at the boundary with the ocean, and with higher resolution in proximity of the coast, to represent horizontal geomorphological gradients in more detail. Finally, to handle complex geometries, such as estuaries and lagoons with intricate channels, curvilinear grids can be used.

10.1.1.4 Vertical Coordinates

Presently, MOHID can handle different vertical coordinates: Sigma, Cartesian, Lagrangian (based on Sigma or based on Cartesian), "Fixed spacing", and Harmonic (Fig. 10.2). These coordinate systems can be used individually or in a combination. Cartesian coordinates are adequate when the flow is horizontal. Harmonic coordinate are similar to the Cartesian coordinate, with the main difference being that the horizontal faces close to the surface expand and collapse depending on the variation of the surface elevation. The sigma coordinates are expressed as a percentage of the total depth, and are convenient when the pressure gradient is barotropic. The Lagrangian coordinates can act as sigma and Cartesian, because it moves the upper and the lower faces of the volume element with the vertical flow velocity.

10.1.1.5 Eulerian and Lagrangian Approaches

MOHID can handle both Eulerian and Lagrangian approaches. The Eulerian approach is implemented by defining a point in a flow field (x, y, z), and by observing how the properties (e.g., velocity, phytoplankton, temperature) change as the fluid passes through this specific location. This approach is the most used in fluid mechanics, because it enables to produce high-resolution pictures of water properties in a given region. The use of the Eulerian approach can prove difficult to label water masses and to monitor their position from the origin over space and time, whereas in the Lagrangian approach, particles can be labelled with information about their releasing point or origin. MOHID's Lagrangian module uses the concept of lagrangian tracers. The most important property of a tracer is its position (x,y,z). A tracer can be a water body, a sediment particle, a group of organisms, or a molecule. The movement of the tracers can be influenced by the velocity field, by the wind, and by random component of velocity. Fecal coliforms can be considered as tracers, and their movement can be tracked down to identify and assess fecal contamination of coastal waters (Sect. 10.2.3). Water masses can be labelled at their origins, and their movement can be tracked down over time. This feature enables to calculate residence time of water in estuaries and bays (Sect. 10.2.4). Oil particles coming from accidental spills can also be labelled and tracked, enabling to assess their displacement over time.

10.2 Advanced Applications with MOHID

10.2.1 Downscaling: From the Large Scale to the Local Scale

In this section, the concept of downscaling is introduced, as a technique to provide boundary conditions from regional to local scale models. Advanced applications of this concept are presented for the Portuguese Coast Operational Model. Operational models are traditionally used in the field of regional oceanography for ocean forecasts and do not include the necessary spatial detail to answer water quality management questions on the local scale. For this reason, downscaling techniques are used to transfer information from regional to local models, enabling a comprehensive description of hydrodynamics and water quality processes. Furthermore, these techniques enable to extend the operational forecasts to the local scale as well.

The idea of downscaling consists of simulating hydrodynamics and water quality on a local scale, based on information provided by larger-scale models. The geographic area covered by a model is named as domain. A domain included inside the domain of another model is named as nested domain, or subdomain. A domain can have one or more subdomains. Models with larger domains are called father models, and provide boundary conditions to their nested models, named as son models. Son models are used to represent estuaries, harbors, and lagoons at a spatial resolution higher than this of the father model.

In the last years, downscaling techniques have been successfully applied in the field of coastal oceanography to simulate hydrodynamics and water quality, and to solve common management questions on the local scale (Leitão et al. 2005; Ascione Kenov et al. 2012; Mateus et al. 2012b). However, the application of these techniques is challenging because it requires reliable and consistent atmospheric and oceanic boundary conditions. Measured data are often difficult to retrieve for the description of boundary conditions. For this reason, meteorological models and large scale ocean models are used to provide boundary conditions to regional models. Additionally, operational modeling requires that model forecasts are timely available to be analyzed by coastal managers and decision makers. This aspect poses additional challenges such as the need to reduce simulation time and the need to simulate several nested domains.

When several nested domains are used, the simulation time is defined by the innermost domain, usually the one with higher spatial and temporal resolution, corresponding to the slower model.

PCOMS is a 3-D hydro-biogeochemical model of the Iberian Western Atlantic region (Fig. 10.3). This model was implemented by MARETEC at IST, Lisbon, Portugal. Ocean boundary conditions are provided by the Mercator-Ocean PSY2V4 North Atlantic and by tidal levels computed by a 2-D version of MOHID, forced by FES2004, and running on a wider region (Mateus et al. 2012b). PCOMS has a horizontal resolution of 6.6 km and a vertical discretization of 50 layers with increasing resolution from the sea bottom upward, reaching 1 m at the surface. Atmospheric forcing is provided by Penn State–NCAR fifth-generation Mesoscale

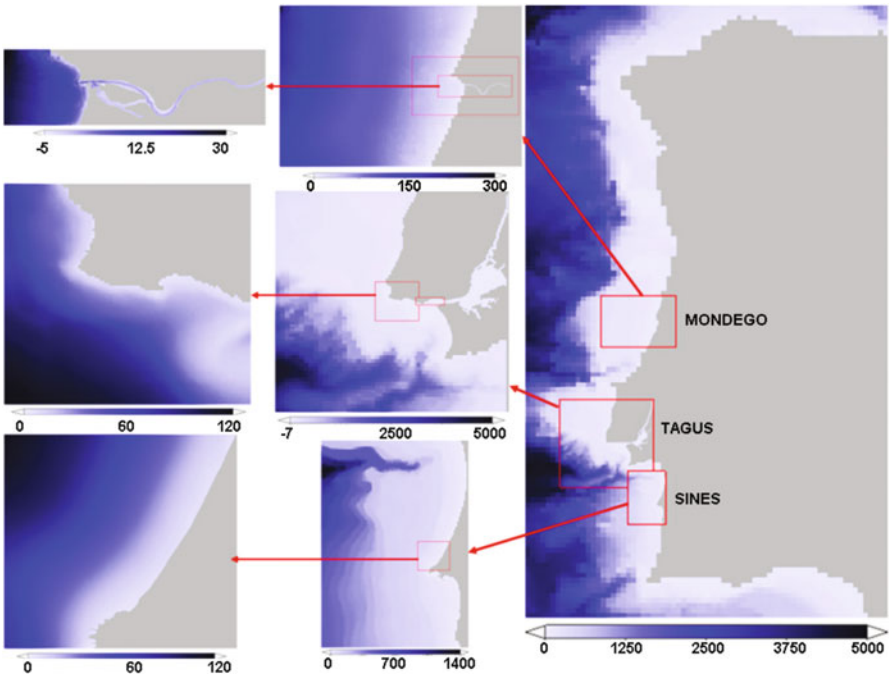

Fig. 10.3 Examples of local models nested in PCOMS. Local applications are systems of nested models, obtained by downscaling the solution of the regional model from 6.6 km up to a 100 m resolution

Model (MM5) (Grell et al. 1994) with a resolution of 9 km (http://meteo.ist.utl.pt). PCOMS integrates different spatial scales and different sources of forcing and boundary conditions, thus improving local-scale model results.

Presently, PCOMS includes several nested models to simulate hydrodynamics and water quality of Portuguese estuaries and coastal areas, including Tagus, Mondego, Ria de Aveiro, and Douro estuaries, among others. Examples of models nested in PCOMS are indicated in Fig. 10.3.

To reduce the simulation time, a delayed mode (offline) technique was designed for PCOMS: the Window Downscaling Technique (WDT). This technique consists of saving model results as pre-defined windows containing results extracted from the regional model of the Portuguese coast. These windows have high temporal resolution, 900 s, enough to represent the main processes coming from the open ocean including the tide signal. The spatial domain of the window must be larger than this of the nested domain. Once the father model simulation is concluded, a window is loaded and applied to a nested model. The described technique enables to run the local model independently, saving time and minimizing redundancy, while improving results. This technique also does not affect the running time of the father domain and enables simultaneous nested model simulations. The WDT enables to nest any coastal or estuary model located in the Portuguese continental zone. An example of nested model is the Tagus estuary, presented in Fig. 10.4 and described in Sect. 10.2.2.

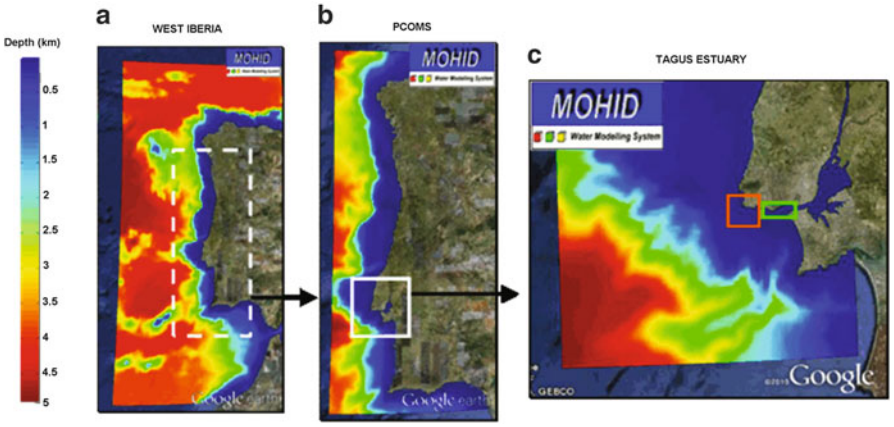

Fig. 10.4 Nested domains used to implement the Tagus model. The domain on the left (**a**) provides tidal boundary conditions to the PCOMS model (**b**), which supplies hydrodynamic and bio-geochemical boundary conditions to the Tagus model (**c**). This model also provides boundary conditions to high resolution local models such as the Tagus mouth (*yellow box*), the Estoril coast model (*green box*), described in Sect. 10.2.3, and the Guia outfall model (*orange box*) (color figure online)

10.2.1.1 Automatic Running Tool

An Automatic Running Tool (ART) was developed to handle preprocessing, running, and post-processing of MOHID simulations, including storing, plotting, and distribution of model results via OPeNDAP, smartphone, and Web pages (Fig. 10.5). The results of the PCOMS and nested models can be found as published maps at http://forecast.maretec.org/.

During the pre-processing phase, ART adapts different data sources to the model domain, including atmospheric model data sources, global circulation model results (i.e. Mercator-Ocean, http://www.mercator-ocean.fr), and measured data from monitoring stations. Atmospheric data sources include MM5 and WRF (Weather Research and Forecasting Model, http://www.wrf-model.org) models.

ART enables running models in a cascade scheme, where son models are waiting for a signal indicating that the father model simulation is concluded. This signal triggers the next model simulation, reducing the time requested for preprocessing. Furthermore, different models can run in different computers at the same time.

10.2.2 The Tagus Operational Model

This section describes a modeling application used to study water quality of the Tagus estuary, Portugal. The modeling application is nested in PCOMS by using the downscaling concept described in Sect. 10.2.1. The geographic domain of the

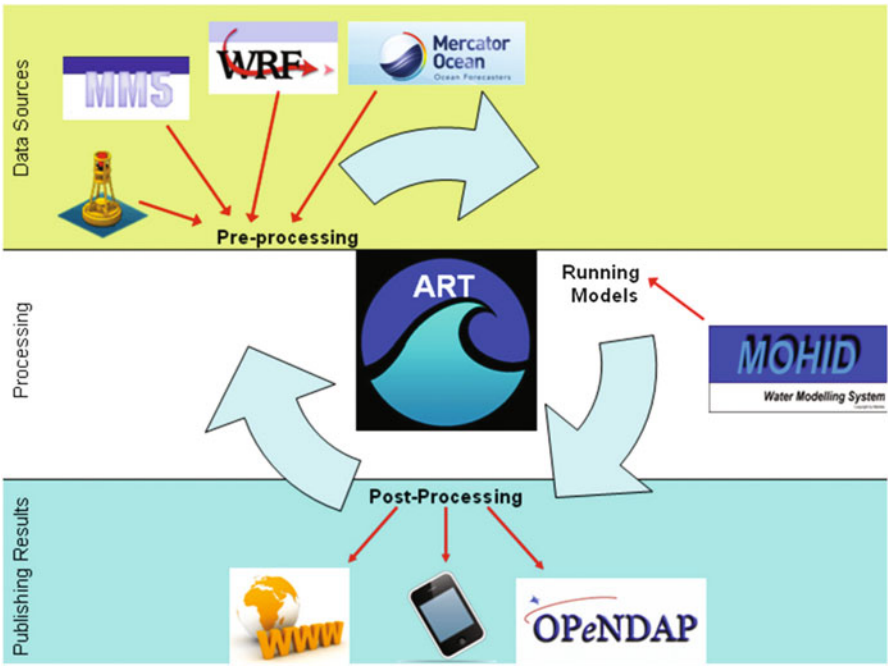

Fig. 10.5 General scheme of the Automatic Running Tool (*ART*)

Tagus model is indicated in Fig. 10.4 (white box). The Tagus estuary is the largest in Portugal and one of the largest estuarine systems in Europe. More than 2.5 million people (25 % of the total Portuguese population) live on the margins of this estuary, with the highest density in Lisbon, the Portuguese capital.

Following the delimitation of the Water Framework Directive (2000/60/EC), the Tagus estuary covers an area of 368 km^2, with an average volume of about 2,700 hm^3. The estuary is mesotidal, dominated by semidiurnal tide. Freshwater inflows are coming mainly from the rivers Tagus, Sorraia, and Trancão (Fig. 10.6). The Tagus River provides the main freshwater input to the estuary. Freshwater inflows data were retrieved by the Portuguese National Information System of Water resources (SNIRH – www.snirh.pt). According to data from the Almourol hydrometric station (39.28°N, −8.22°E) for the period 1973–2012, the annual mean freshwater inflow is 300 m^3s^{-1}. The average and the maximum water fluxes in summer are 100 m^3s^{-1} and 400 m^3s^{-1}, respectively. In winter, the average and maximum fluxes are 700 m^3s^{-1} and 3,500 m^3s^{-1}, respectively. Sorraia and Trancão, the other two most important tributaries, have an annual mean flow of 39 m^3s^{-1} and 6 m^3s^{-1}, respectively. The bathymetry of the Tagus estuary, shown in Fig. 10.6, was generated by merging data collected during several bathymetric surveys, and provided by the Portuguese Hydrographical Institute (www.hidrografico.pt/).

MARETEC has a 3-D hydro-biogeochemical operational model for the Tagus estuary since 2011. The horizontal resolution ranges from 2 km in the ocean to

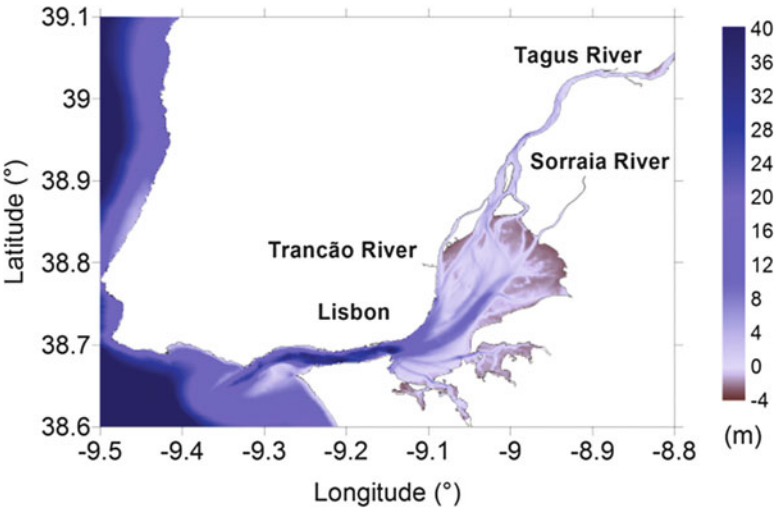

Fig. 10.6 Bathymetry of the Tagus estuary. Depths are referred to the hydrographic zero, set to 2.08 m below the mean sea level. The areas with negative depths are intertidal zones, which are emerged during low tides

300 m around the estuary mouth. The vertical discretisation consists of 43 Cartesian layers overlapped by seven Sigma layers. The vertical resolution is about 1 m near the water surface. Boundary conditions are provided by PCOMS (Sect. 10.2.1). The atmospheric forcing is provided by WRF model results produced at IST with a 3 km resolution (http://meteo.ist.utl.pt/).

In 2013, a new subdomain was developed inside the Tagus estuary operational model. This subdomain has a horizontal resolution of 200 m and covers the mouth and the inner part of the estuary. The vertical discretisation is the same as the one of the father domain. The two nested domains of the Tagus estuary operational model are shown in Fig. 10.7.

The Tagus operational model currently produces daily results and 48 h forecasts. Every day, the forecast of the previous day are simulated again, by using the best ocean boundary conditions and atmospheric forcing available, and hourly freshwater inflow measurements from the Almourol hydrometric station. The discharges of biogeochemical properties are defined upstream of the Tagus River by using climatological data. For Sorraia and Trancão rivers, both freshwater river inflow and biogeochemical properties discharges, are defined by using climatological data. Average discharges from urban waste water treatment plants are included in the model as well. Apart from the hydrodynamic results (currents and water level), the Tagus estuary operational model generates forecasts for the properties described in Table 10.1.

The Tagus model is used to assess the complex dynamic of the water properties in the estuarine system, including the cohesive sediment transport. Simulated velocity modulus and cohesive sediment concentrations during one tidal cycle are

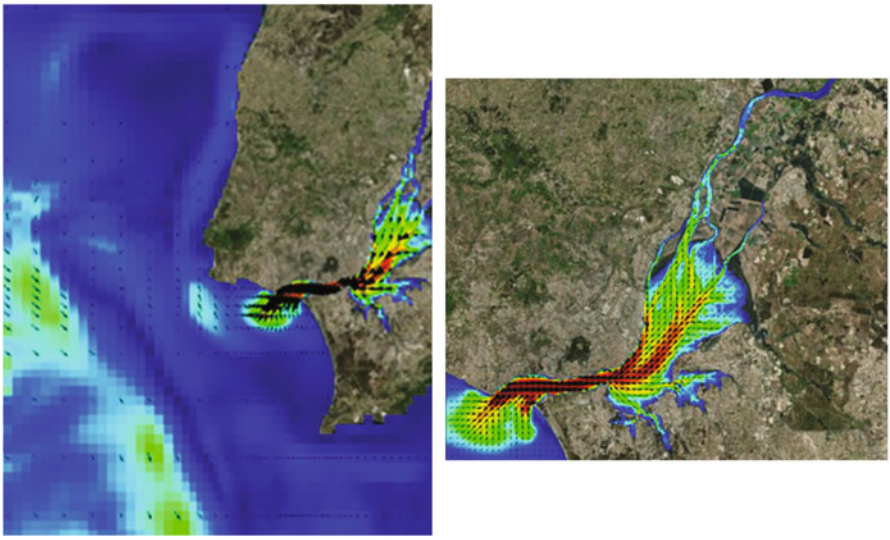

Fig. 10.7 The two domains of the Tagus estuary operational model. The horizontal resolution ranges from 2 km in the ocean to 300 m around the estuary mouth in the first domain (*left*). The second domain has a constant horizontal resolution of 200 m (*right*)

Table 10.1 Properties simulated by the Tagus estuary operational model

Water properties
Salinity
Temperature
Dissolved oxygen
Cohesive sediments
Phytoplankton
Zooplankton
Ammoniacal nitrogen
Nitrate
Nitrite
Refractory dissolved organic nitrogen
Non-refractory dissolved organic nitrogen
Particulate organic nitrogen
Inorganic phosphorous
Refractory dissolved organic phosphorous
Non-refractory dissolved organic phosphorous
Particulate organic phosphorous

shown in Figs. 10.8 and 10.9, respectively. The results show cohesive suspended sediments are eroded from the bottom when the velocities are high. The currents carry upstream the cohesive suspended sediments during flood tide, and downstream during ebb tide. The cohesive sediment concentrations in water decrease in the slack tide period, when the deposition rate is the highest, due to low velocity intensities.

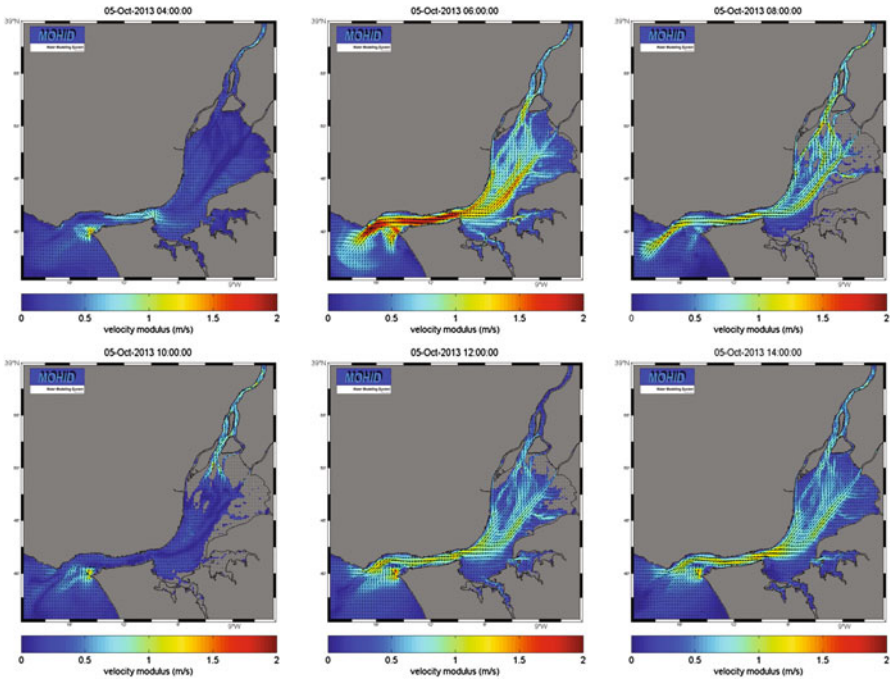

Fig. 10.8 Velocity modulus in the Tagus estuary during one tidal cycle

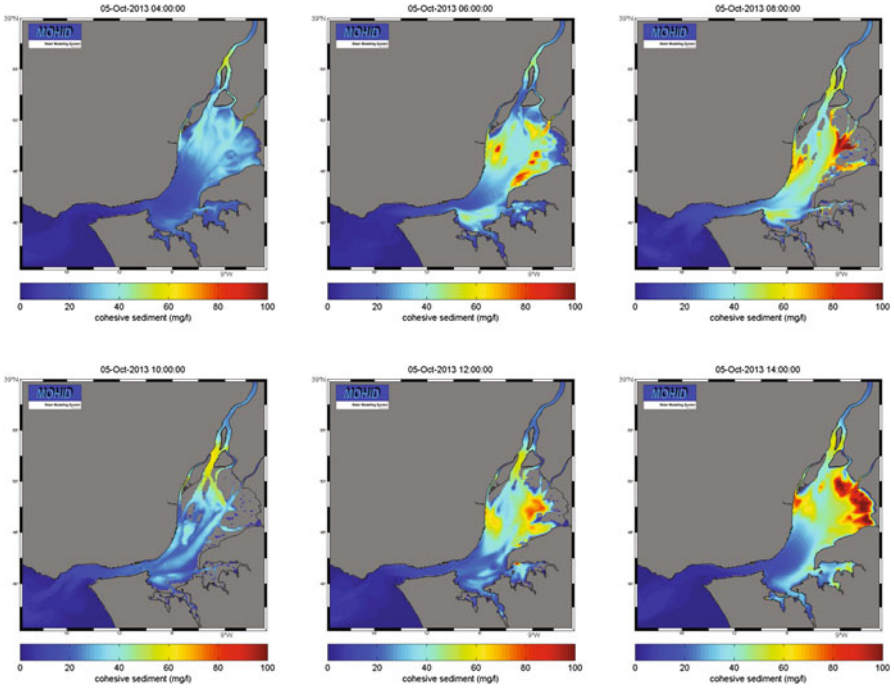

Fig. 10.9 Cohesive suspended sediments in the Tagus estuary during one tidal cycle

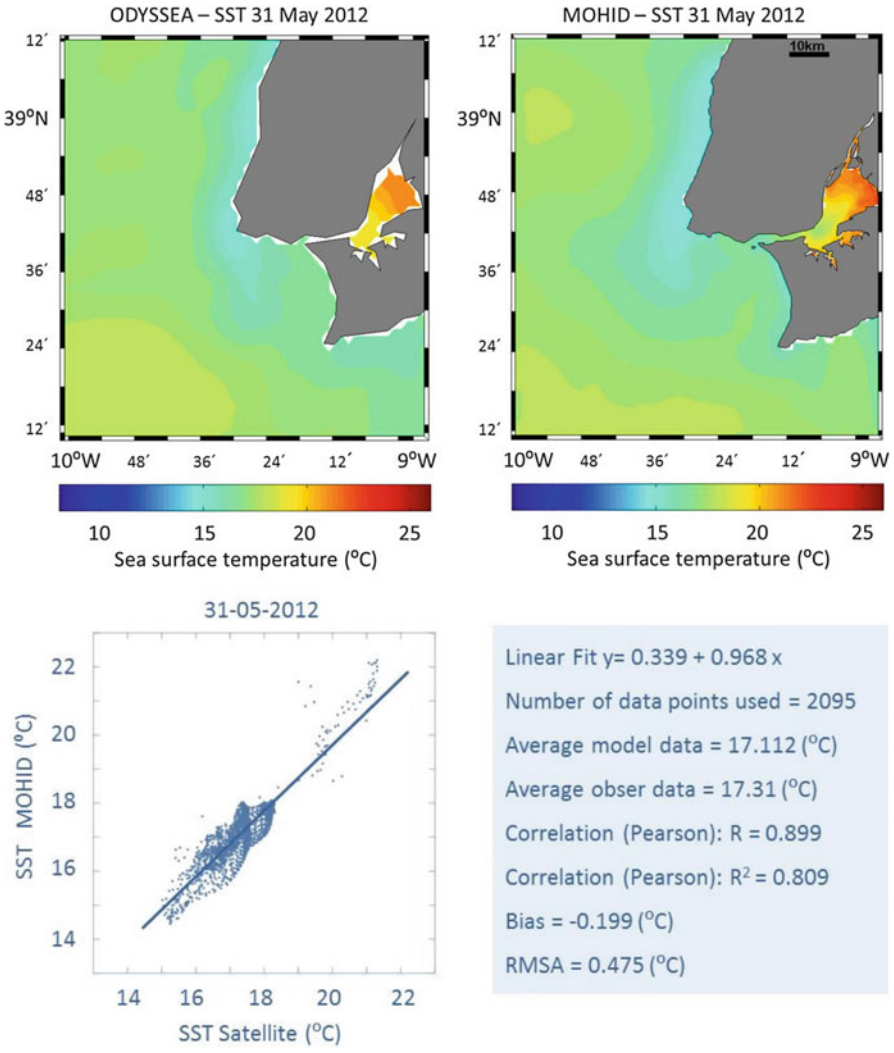

Fig. 10.10 Remote sensing data for sea surface temperature (*left panel*) and model predictions (*right panel*) for 31 May 2012

10.2.2.1 Model Validation

The validation of the Tagus estuary model relies on both satellite images and in-situ data from moored stations in the inner estuary and monitoring programs in the coastal adjacent area. An example of modeled surface temperature validation with remote sensing data is presented in Fig. 10.10 for May 2012. A simple comparison of both figures shows a remarkable resemblance, denoting that the model is able to reproduce some of the major physical patterns in the estuarine and coastal areas,

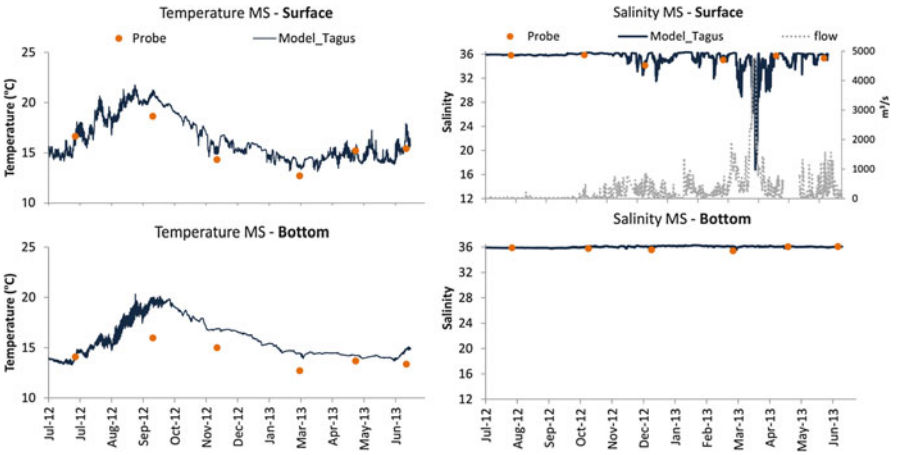

Fig. 10.11 Model results (*line*) and field data (*markers*) for temperature and salinity at different depths for a monitoring station located in the adjacent area of the Tagus estuary (Station MS in Fig. 10.10), from July 2012 to July 2013

such as, the cold water mass near the coast as a result of upwelling, and the higher temperature waters inside the estuary.

Field data retrieved with multi-parameter probes or discrete samples (3 depth levels) during monitoring programs provide a description of the vertical structure in the coastal area around a submarine outfall. Monitoring programs, however, have significant limitations in the temporal characterization of the processes, although they are important nonetheless because they can provide a view of the tri-dimensional structure of the estuarine adjacent area, where strong horizontal and vertical gradients are usually found. Figures 10.11 and 10.12 illustrate the model validation with in-situ data for surface and bottom depth levels. The comparison of simulated and measured temperature, salinity, nitrate and chlorophyll concentrations shows good fit, with model results following the seasonal trend seen in field data.

These examples of estuarine model validation denote the advantages of comparing field data with model results, but also expose some of its limitations. Modelers trying to validate their models of such dynamic systems must bear in mind the existence of discrepancy between the spatial and temporal resolution of both data sets; while model results cover fully the studied domain and can have small temporal resolutions, in-situ data sets are usually scarce because of methodological and equipment constraints, and an intrinsic economic restrictions in the monitoring programs. If temporal and spatial coverage of field data is too sparse for the scales of the processes, the comparison of such data sets must be made on a qualitative, rather than quantitative, basis. The ability of the model to reproduce general features such as seasonal trends and major vertical patterns, as in the case presented in Figs. 10.10 and 10.11, stand as a good example of validation that can be attained in such cases.

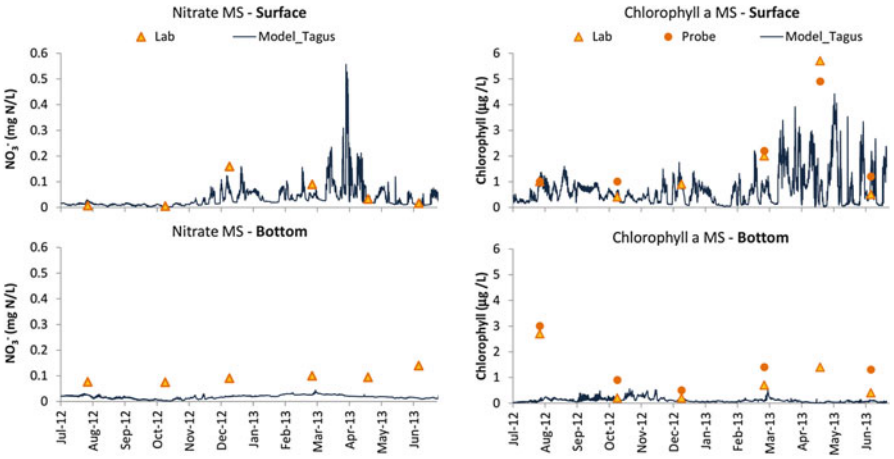

Fig. 10.12 Model results (*line*) and field data (*markers*) for nitrate and chlorophyll-a at different depths for a monitoring station located in the adjacent area of the Tagus estuary (Station MS in Fig. 10.10), from July 2012 to July 2013

10.2.3 Bathing Water Quality

This section describes a modeling application used to study bathing water quality (BWQ) of the Estoril coast, located in proximity to the Tagus estuary, Portugal. An operational model was implemented to provide daily BWQ forecasts. The model was used to simulate and study contaminant plume dispersion along the coastline. Using the Lagrangian methodology and automatic hydrometric data from four streams discharging in the area, the model simulated streams discharges (that can have fecal contamination), and provided BWQ forecast. The model configuration was based on an implementation originally developed by Fernandes (2005) and used in several studies of the Tagus Estuary (Fernandes et al. 2006; Campuzano et al. 2010, 2012; Pinto et al. 2012).

The model included three nested domains. The first domain is PCOMS (Sect. 10.2.1). The second domain (Fig. 10.13b) is the Tagus estuary model described in Sect. 10.2.2, which provided hydrodynamic fields, and density gradients (temperature and salinity) to the next level. The third domain (Fig. 10.13c), included the area between Carcavelos and Belém, on the Estoril coast (from −9.356°W to −9.2285°W and from 38.669°N to 38.705°N). The model was implemented by using a 3-D configuration, with a constant horizontal spatial step of 30 m (460 × 120 cells), and a time step of 6 s. The vertical geometry included seven sigma layers between the surface and 8.68 m, and five Cartesian layers between 8.68 and 35 m (maximum depth).

Atmospheric forcing was provided by MM5 and WRF models (3 km resolution) (www.meteo.ist.utl.pt), including wind (modulus and direction), air temperature, relative humidity, solar radiation and wind stress.

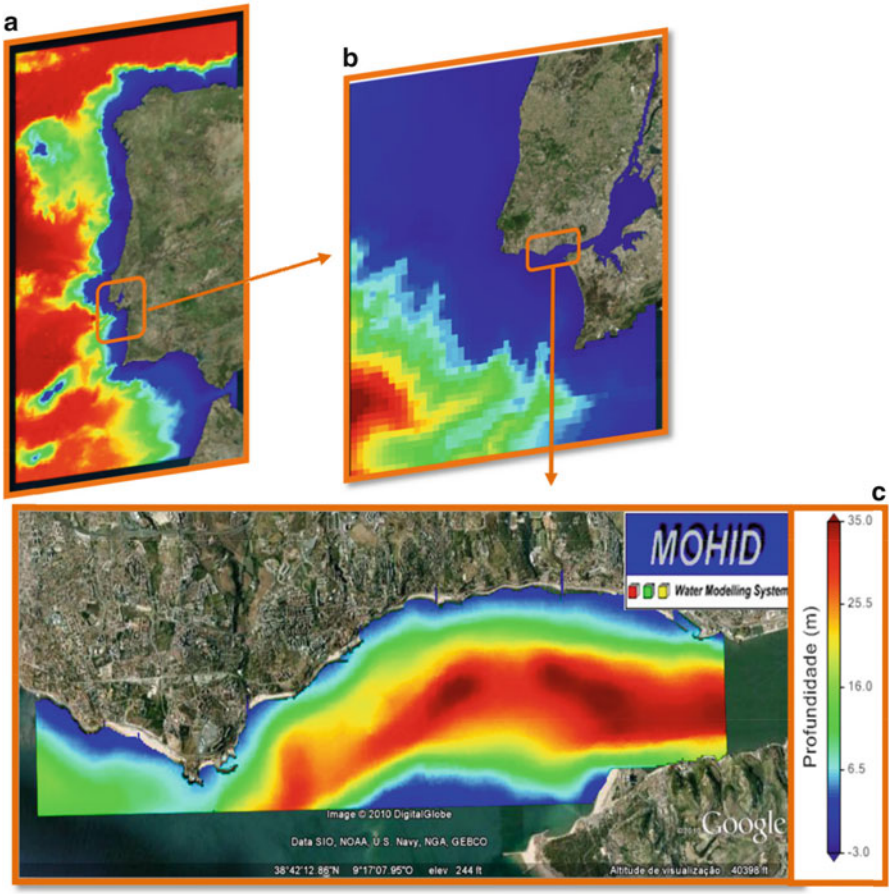

Fig. 10.13 Nested domains. (**a**) PCOMS, (**b**) Tagus, and (**c**) Estoril coast

Freshwater discharges were obtained from historical data and INAG[1] automatic stations (in Jamor), SANEST[2] and IST stations (in Sassoeiros, Marianas, Lage and Barcarena streams). The automatic stations were used to collect daily hydrometric levels which were converted into stream discharges, using level/discharge gauges. Due to the lack of up-to-date information, discharges for Algés, Junça, and Porto Salvo streams were estimated from historical data.

The lagrangian model was coupled to the hydrodynamic model, to simulate stream discharges and their effect on the beaches. After the hydrodynamic simulation was carried out, model results were stored at a high temporal resolution. Using

[1] INAG - Instituto da Água, http://www.apambiente.pt

[2] SANEST - Saneamento Costa do Estoril, http://www.sanest.pt

an off-line method, Lagrangian transport was efficiently and rapidly computed by using previously generated results of the hydrodynamic model.

10.2.3.1 Fecal Decay Model

The model assumed that fecal bacteria do not reproduce in the aquatic environment and that their decay is linear. The bacteria concentration c is described by a first order equation:

$$\frac{\partial c}{\partial t} = -kc \tag{10.4}$$

The mortality rate k was computed as a function of solar radiation intensity, salinity and temperature based on Canteras et al. (1995) and described in Viegas et al. (2012).

10.2.3.2 Bathing Water Quality Assessment

The new European Bathing Water Directive (NBWD) classifies BWQ by using maximum thresholds and exceeding probability. If the maximum threshold is respected for longer than 90 % of the time water is "acceptable" and if it is respected for longer than 95 % of the time, water is classified as "excellent". These percentages can be read as "the probability of a bather to be in bathing water complying with the maximum threshold". This probability is measured as the probability of weekly sampling compliant water in a fixed point assumed as representative of the whole bathing water.

To assess BWQ it was necessary to define the area of bathing water, to identify polluted water masses inside the bathing water (and their origin), and to calculate bulk concentration of the bathing water. The spatial distribution of bathing waters was defined by dividing the study area into sub-areas considered as monitoring boxes, following the methodology described in Braunschweig et al. (2003) for tracking water masses and for the computation of water residence time. A bathing water was defined as the monitoring box delimited by the beach line and with its cross dimension in the order of the swimming length (up to 200 m).

To identify polluted masses inside bathing water, the tracers were labelled by their origin, in such a way that their position at any time instant could be linked to their release points (origins). At each time step, the model calculates the volume of each monitoring box and the volume of the tracers inside each monitoring box. The contamination probability was computed as the ratio between the volume of contaminated water and the volume of the monitoring box. The fecal contamination was quantified trough the geometric mean of all contaminated tracers in each monitoring box. To simulate the plume of each pollution source, twenty Lagrangian

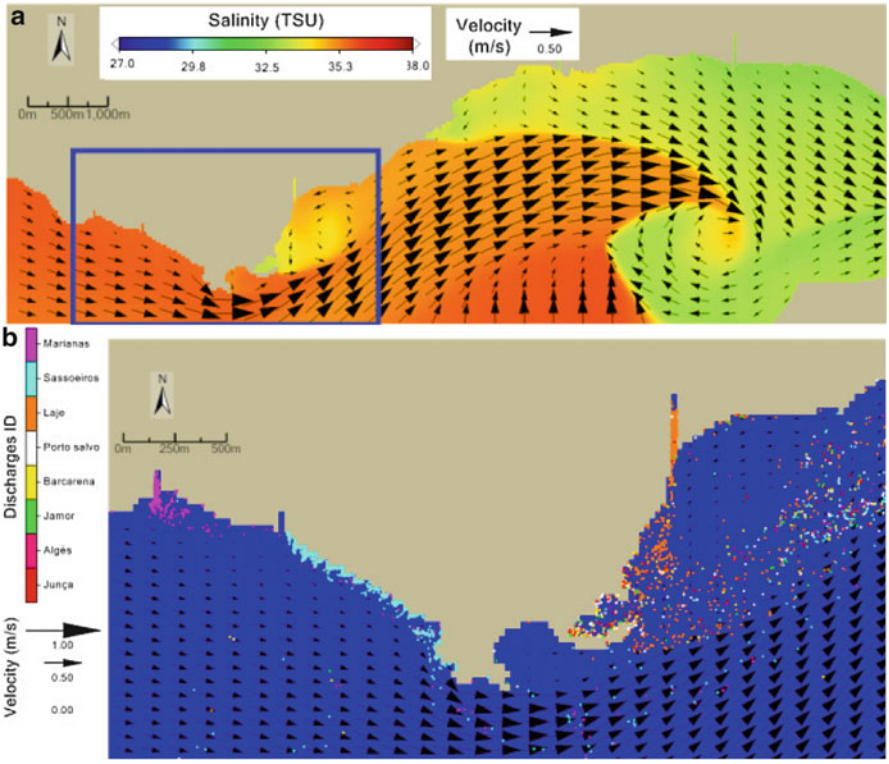

Fig. 10.14 Salinity and velocity fields for Estoril Coast domain during flood tide (**a**), and a detailed image for bathing waters for the same time with lagrangian tracers representing stream discharges ID with different colours (**b**)

tracers were released per minute, at each discharge point (Fig. 10.14). The load associated to tracers released at the mouth of a stream under normal conditions was obtained by using the geometric average of historical data.

The average concentration in a generic monitoring box "x" was calculated as:

$$C_x = 10^e \tag{10.5}$$

$$e = \frac{\sum_{NPollutedTracers} \log C_i}{NPollutedTracers} \tag{10.6}$$

C_i is the concentration of a tracer computed as the ratio between the number of bacteria transported by the tracer and its current volume Vol_i. Tracers were considered polluted if their fecal contamination reached the NBWD limit of 102UFC/100 ml. *NPollutedTracers* is the number of polluted tracers.

The probability P of a bather to be in contact with polluted water was computed as the ratio between the total volume of polluted tracers and the volume of the monitoring box "x":

$$P = \frac{\sum_{NPollutedTracers} Vol_i}{Vol_x} \tag{10.7}$$

Finally, contamination risk was evaluated by combining (1) fecal contamination, and; (2) the probability of a bather to be in contact of contamination water. The bathing water was considered contaminated if:

- the concentration was above the maximum threshold, and;
- the probability of a bather to be in contact with that water was above 1 %.

To estimate contamination risk, the probability results were analyzed at intervals of 3 h, considering the maximum probability value of each interval. Following this methodology, it was possible to predict the contamination probability in bathing water (Viegas et al. 2012).

The proposed methodology enables the answering of common management questions related to BWQ such as:

- Is there contaminated water in bathing water? What is the concentration?
- What is the probability of a bather being exposed to such that water?
- What is the origin of the contamination?

The methodology was applied, tested, calibrated and validated, during the 2011 and 2012 bathing seasons. Results showed that the Lagrangian model approach using the box methodology was able to forecast the contamination risk in the bathing water, and to predict fecal contamination. The proposed methodology also enabled the identification and quantification of contaminant plume, the identification of major pollution sources, and the establishment of minimization or mitigation actions.

Model simulations evidence the temporal and spatial variability of fecal contamination, revealing the importance of using modeling tools to explain and predict bathing water quality. For the performed tests, the modeling system was crucial to estimate the probability of the bathers being in contact with contaminated water. Results evidence the role of the local hydrodynamic fields on the stream plumes distribution along bathing waters, showing that contamination risk and values can change during the day on the same beach.

The implemented risk prediction methodology allows responding to NBWD statements, giving timely predictions about short-term pollution events, when they occur after raining events, or water level rising in streams. With the implementation of this methodology beach managers can predict the risk of contamination events, prevent bathers from being exposed to pollution, and in accordance with bathing water profile definition (IST and SANEST 2004; Viegas et al. 2009; Neves et al. 2010; Leitão et al. 2012) to minimize by up to 15 % the use of monitoring samples. This methodology was applied to specific bathing waters, but it can be implemented to other coastal areas around the world.

10.2.4 Residence Time of Water

This section describes a modeling application used to calculate the residence time of water in the Mondego estuary, Portugal. To implement the model of the Mondego estuary, four domains were nested inside PCOMS by using downscaling concept described in Sect. 10.2.1. The geographic area of the four domains is indicated in Fig. 10.3.

Residence time of water is the average time that a water parcel spends inside a system such as an estuary, a harbor, or a lagoon (Braunschweig et al. 2003). The residence time of water provides useful information in estuarine water quality studies because it can be used to determine for how long discharged pollutants will remain in the system before to be flushed away. Numerical models often contain advanced tools to calculate residence time of water (Braunschweig et al. 2003; Choi and Lee 2004; Cucco and Umgiesser 2006; Ascione Kenov et al. 2012). MOHID includes tools to calculate residence time of water by using Lagrangian models coupled with 2-D and 3-D hydrodynamic models. The methodology used in MOHID to calculate residence time of water in estuaries is divided into four steps (Braunschweig et al. 2003; Ascione Kenov et al. 2012):

- The estuary is divided into sub-areas, named as boxes, characterized by similar geomorphology and hydrodynamics;
- The boxes are filled with Lagrangian tracers in such a way that the volume of the tracers matches the total volume of the estuary;
- The Lagrangian tracers are transported out of the estuary by currents;
- The residence time of water is computed as the time required for 80 % of the initial tracers to leave the estuary.

The methodology enables to calculate water residence time of the whole estuary and of the single boxes as well. Each tracer is identified by its own origin, so that for a given water mass at a point x and at a time t it is possible to know from where the particle was released. Using the Lagrangian approach, the water fraction f_{ij} inside a box i at a time instant t with origin from box j is calculated as (Eq.10.8):

$$f_{i,j}(t) = \frac{V_{i,j}(t)}{V_{i,i}(0)} \tag{10.8}$$

$V_{ij}(t)$ is the volume of tracers released in box j, present inside box i at time t, and $V_{i,i}(t=0)$ is the water volume in box i at the beginning of the simulation. By integrating the water fraction and normalizing it by time, the integrated water fraction is obtained:

$$F_{i,j}(T) = \frac{1}{T}\int_0^T \frac{V_{i,j}(t)}{V_{i,j}(0)}dt \tag{10.9}$$

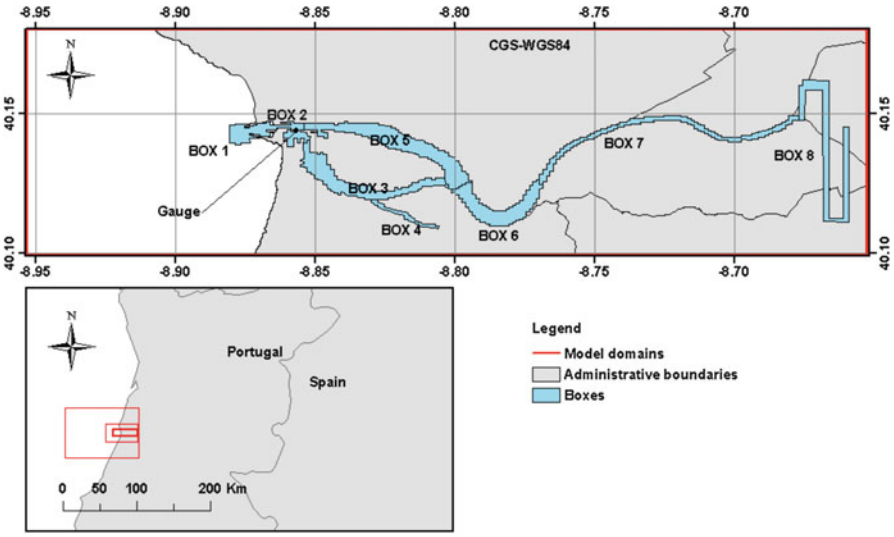

Fig. 10.15 Geographic location of the Mondego estuary. Boxes, model domains, and velocity gauges are indicated as well

The parameter $F_{i,j}$ in Eq. 10.9 measures the integrated influence of box j over box i during the time T. For the special case $i = j$ this parameter is related to the residence time of water. At the beginning of the simulation, F is equal to 1. As water is renewed, the contribution of the initial water to the total volume of the box decreases and F tends to 0. The time at which $F = 0$ is the residence time of water. However, in estuaries characterized by tidal influence, some of the water particles remain trapped inside intertidal areas and never leave the box. For this reason, following Braunschweig et al. (2003), the residence time of water is considered as the time at which 80 % of the tracers have already left the box. The same concept used for a box is applied to calculate the residence time of water for an estuary.

10.2.4.1 Residence Time of Water in the Mondego Estuary

The Mondego Estuary (40.15°N, −8.85°E) is located on the Portuguese Atlantic coast, and it is divided by the Murraceira Island into two arms (Fig. 10.15). The northern arm has depths varying with tides (between 5 and 10 m during flood tide, with respect to mean sea level), and receives water inflows from the Mondego River. The southern arm is characterized by lower depths compared to the northern arm (between 2 and 4 m during flood tide, with respect to mean sea level), and receives water inflows from the Pranto river. The tidal range varies between 0.35 and 3.3 m with respect to the mean sea level. Freshwater inflows range between 800 m^3/s in the winter and 10 m^3/s in the summer. To calculate water residence time, the estuary was divided into boxes. These boxes were filled with Lagrangian

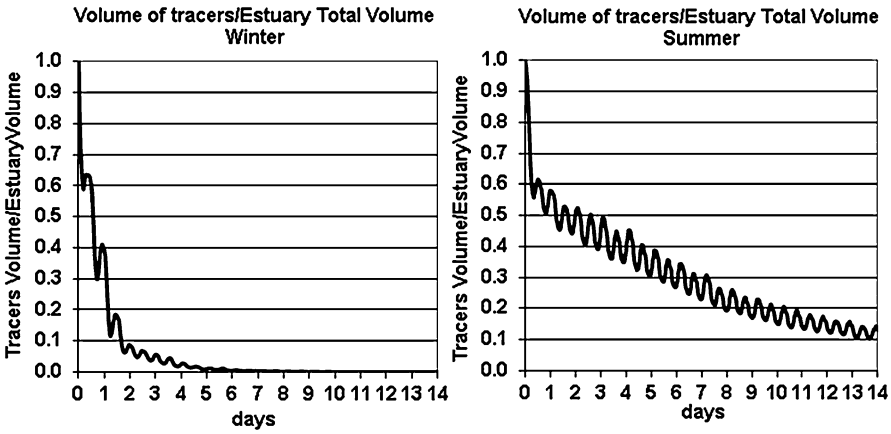

Fig. 10.16 Temporal evolution of the ratio between the tracers' volume and the estuary volume in winter and in summer

tracers, in a way that the total volume associated to the tracers matched the total volume of the estuary. The boxes were used both to release tracers, and to monitor the path of the particles passing through them. Each tracer was identified by its own origin, so that for a given water mass at a point x and at a time t it was possible to know from where it was released.

The evolution of the tracers' fraction in the estuary was calculated by considering river inflows in winter and in summer. The model was forced by using atmospheric data provided by the MM5 model (http://meteo.ist.utl.pt) at a resolution of 3 km. River upstream freshwater inputs were defined by using daily freshwater inflows from the database of Portuguese National Hydrological Service (SNIRH-www.snirh.pt).

For modeling the hydrodynamics in the estuary, the downscaling technique described in Sect. 10.2.1 was used. A model configuration was used with four domains nested in PCOMS (Fig. 10.3), to transfer boundary conditions from the regional to the local scale.

PCOMS provided fields of velocity, temperature, salinity and water levels with a fixed resolution of 6.6 km. The results of the hydrodynamic model were validated by comparing simulated and measured velocities collected by the buoy of the SIMPATICO monitoring system, located in the estuary at 40.14°N −8.85°E. Model implementation is described in Ascione Kenov et al. (2012).

The ratio between the volume of the tracers and the volume of the river is described in Fig. 10.16. This ratio decreases over time, indicating that the water is gradually renewed. The distribution of lagrangian tracers is described in Fig. 10.17. The results showed that the residence time of water was about 1 day in winter, and about 9 days in summer. This result is explained by the seasonal variation of the freshwater inflows, which values are usually higher in winter than in summer. The tide did not show a relevant effect on water renewal, concluding that the freshwater inflow was the main factor affecting water residence time in the study area.

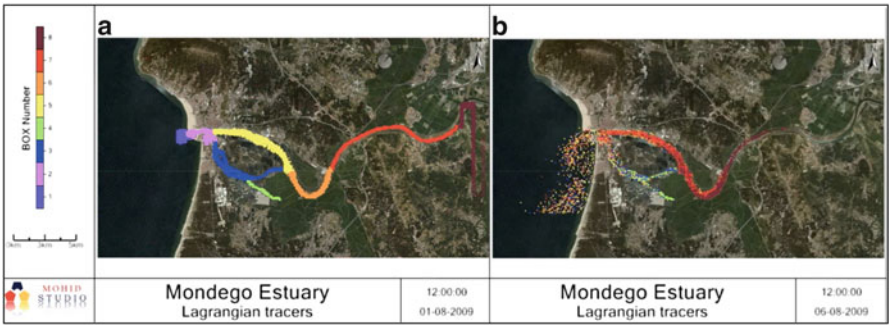

Fig. 10.17 Spatial distribution of Lagrangian tracers at the beginning of summer simulation (**a**) and after 6 days (**b**)

10.2.5 Nutrient Exchanges Between Estuaries and the Ocean

A 3-D hydrodynamic-ecological model of the Aveiro coastal area, Portugal, was nested in PCOMS, following the concept of downscaling described in Sect. 10.2.1. The model was used to quantify nutrient exchanges between the estuarine system and the ocean, considering nutrient inputs coming from land and from a submarine outfall.

The nutrient exchanges between estuaries and the ocean influence the trophic status of water bodies because they may affect primary production and oxygen renewal rates. The assessment of nutrient exchanges is challenging because it requires the identification and quantification of diffuse and point sources. Marine eutrophication is often heightened by anthropogenic inputs and the nutrients released by submarine outfalls could trigger algal blooms in coastal areas. The Vouga estuary (hereafter Ria de Aveiro), located on the Portuguese coast (40°N, −9°E), is a mesotidal estuary with a complex morphology and a wide intertidal area. The estuary is considered a high productive system, classified as a "sensitive area" in terms of eutrophication (91/271/EC). Little is known about nutrient fluxes between Ria de Aveiro and the ocean. Main freshwater inputs come from five tributaries (Caster, Antuã, Vouga, Boco and Mira channel). Additionally, nutrients are discharged into the coastal water by the São Jacinto submarine outfall located at a distance of about 3 km from the Aveiro coast. The outfall carries treated wastewater from three wastewater treatment plants and a paper mill, and it has a 300 m long diffuser located at a depth of 17 m. The average depth of the estuary is about 1 m, but in some channels, depths are kept between 4 and 7 m through constant dredging. The estuary's mouth is 350 m wide and about 20 m deep, with a large tidal prism (Dias et al. 2000). The study area is located in the northern part of the northern-hemisphere subtropical high pressure belt, and its climate is affected by the Azores anti-cyclone (Lopes et al. 2009). Due to this high pressure system, winter is dominated by weak southerly and westerly winds. In summer, the atmospheric current is characterized by northerly and north-westerly winds of about 5–6 m/s (Silva et al. 2001).

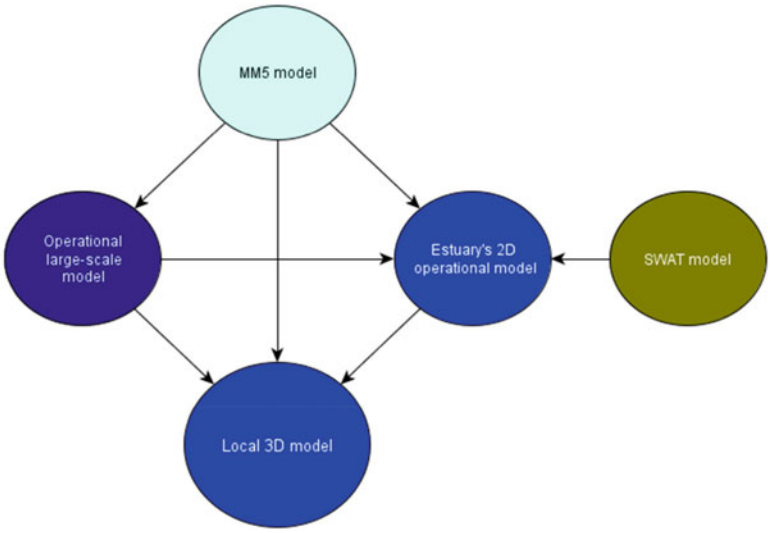

Fig. 10.18 Conceptual scheme of the models used to compute nutrient fluxes between the Ria de Aveiro and the ocean

Three different sources of nutrients were considered: the estuary, the ocean, and the submarine outfall. To account for exchanges between the estuary and ocean, the 3-D model was coupled to a 2-D hydrodynamic-ecological model of the estuary. The 3-D model has a horizontal grid of 1.5×1.5 km resolution (56×48 cells), covering an area of about 2,500 km^2. The 2-D model was used to represent the inner estuary, with a variable resolution between 1 km offshore and 200 m inside the estuary. The 2-D model of the estuary was coupled to the Soil and Water Assessment Tool (SWAT) applied to the Vouga catchment, to account for the exchanges between the land and the estuary. Figure 10.18 shows the conceptual scheme used to integrate the different models and the information flow between them. The simulation covered the period between February and November 2011. The model was validated by comparing model results with satellite images of chlorophyll, and with observed chlorophyll and nitrate concentrations. The spatial variation of nitrate and phytoplankton was characterized by subdividing the study area into boxes (Fig. 10.19). Fluxes of water, nitrate, and chlorophyll between the boxes and the surrounding waters were computed.

Atmospheric forcing was imposed by using the MM5 model results with 9 km resolution (http://meteo.ist.utl.pt). All bathymetries were built from the EMODnet Gridded Bathymetry (EGB) database (http://www.emodnet-hydrography.eu/). The submarine outfall's discharge was implemented as an increment of volume and included flow, nutrient concentrations, temperature and salinity.

The 2-D model simulated hydrodynamics and water quality inside the estuary, providing fields of velocity, temperature, salinity and biogeochemical properties as output over time. Hourly fluxes of biogeochemical properties provided by the 2-D

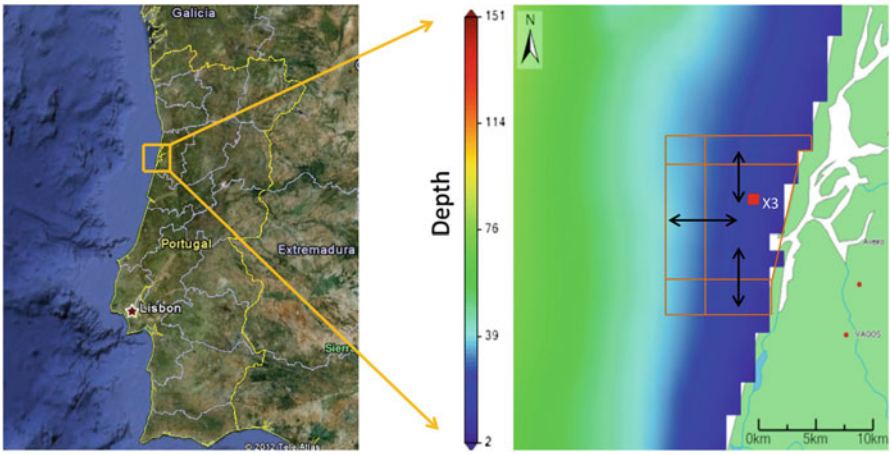

Fig. 10.19 Location of boxes used to compute nitrate and phytoplankton fluxes. The *red square* indicates the location of both the submarine outfall and the monitoring station. The Ria de Aveiro tributaries are indicated as well (color figure online)

model were used to determine nutrient concentrations exiting the estuary. Additionally, the 2-D model provided velocity and direction of the flow exiting the estuary, which was used to calculate the momentum discharge, important for the simulation of the Coriolis effect on coastal hydrodynamics.

To evaluate the importance of the three different nutrient sources (the ocean, the estuary, and the submarine outfall), three different scenarios were built: the first one considered the ocean as the only nutrient source; the second one included the ocean and the estuary, and; the third one included all the three sources.

Results in Fig. 10.20 show the comparison between simulated and measured concentrations of nitrate and chlorophyll at station X3, located close to the submarine outfall and indicated in Fig. 10.19. In this station, the maximum measured chlorophyll *a* concentration was 7 μg/l, with an average value of 2.9 μg/l at the surface and 2.2 μg/l in the bottom waters. Following the classification of the 91/676/CEE directive, these waters can be considered as mesotrophic (<10 μg/l) and yet very close to oligotrophic (<2.5 μg/l). Simulated nitrate concentrations were about 0.019 mg N/l (average values) in surface and bottom waters. Following the same directive, the waters can be classified in the first eutrophication level (0–2 mg N/l).

In overall, measured and simulated nitrate and chlorophyll *a* concentrations showed qualitative agreement. The concentrations of chlorophyll *a* decreased in August and stabilized at the end of the summer. Simulated nitrate concentrations had low agreement with data, with small variations over the simulated period, but almost always below 0.04 mg N/l.

Fluxes of water, nitrate, and phytoplankton between the estuary and the ocean are described in Table 10.2, for the month of July. The directions are taken by considering the box in the mouth of the estuary as a reference point. As an example, Northward in Table 10.2 indicates the direction of the flow going North with respect

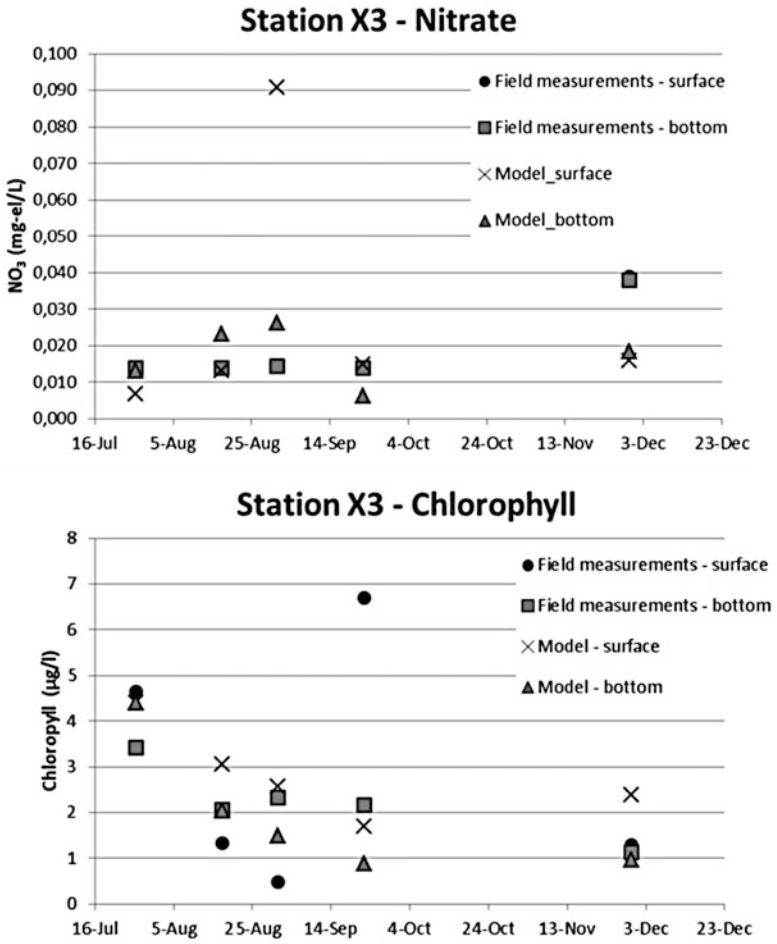

Fig. 10.20 Comparison between simulated and measured concentrations of nitrate and chlorophyll *a* at station X3, located close to the submarine outfall (Fig. 10.19)

to the box in the mouth of the estuary. In the three scenarios the dominant fluxes were from North to South and to West, as expected during upwelling conditions (July).

Results in Table 10.2 show that the estuarine discharge affects the fluxes considerably, with high monthly volume of water carried southward (from $32{,}100 \times 10^6$ m^3 to $35{,}833 \times 10^6$ m^3) and westward (from $15{,}500 \times 10^6$ m^3 to $20{,}220 \times 10^6$ m^3). The results show an increase of phytoplankton fluxes from 4,770 t of carbon in the scenario without estuarine discharge to 5,542 t of carbon in the scenario with estuarine discharge. The nitrate fluxes increase from 81 in the scenario without estuarine discharge to 236 t of nitrogen in the scenario with estuarine discharge. The reason for this increase of flux is directly related to the

Table 10.2 Simulated water, nitrate and phytoplankton fluxes in July 2011

Flux direction	Ocean			Ocean + estuary			Ocean + estuary + outfall		
	Water	Nitrate	Phy	Water	Nitrate	Phy	Water	Nitrate	Phy
	$10^{\wedge 6}$ m^3	ton N	ton C	$10^{\wedge 6}$ m^3	ton N	ton C	$10^{\wedge 6}$ m^3	ton N	ton C
Northward	−32,100	−81	−4,770	−35,833	−236	−5,542	−35,843	−233	−5,535
Southward	16,500	37	2,622	15,599	98	2,418	15,630	103	2,471
Westward	15,500	−18	2,533	20,220	78.4	3,328	20,202	81	3,361

Phy indicates phytoplankton

near-horizontal angle of the discharge, which made the water from the estuary to head West before to be moved northward by the Coriolis force. Results in Table 10.2 show that high fluxes of phytoplankton were associated to low nitrate fluxes in the same direction, because phytoplankton consumes the nitrate. This is particularly evident in the westward direction (main flow direction of the estuary's discharge): high fluxes of phytoplankton are transported westward, and the nitrate along this direction is quickly consumed, resulting in low nitrate fluxes.

The most important result shown in Table 10.2 is the very low contribution of the submarine outfall on phytoplankton and nitrate fluxes. The fraction of the fluxes represented by this source was below 6 % with a maximum of 5.1 % in the southward flux from the estuary's mouth. On the contrary, the Ria de Aveiro was responsible for more than a 31 % increase of nitrate and phytoplankton fluxes. Thus, the estuary can be regarded as the most important source of nutrients in the coastal area. The nitrate concentration contributions from the ocean, the estuary, and the submarine outfall near the estuary's mouth were below 38 %, over 65 % and below 6 %, respectively, which means that near the mouth of the Ria de Aveiro, nitrate fluxes were strongly associated with freshwater discharge. It can be concluded that the submarine outfall has little influence on the fluxes of nitrate and phytoplankton in the Aveiro coast. These modeling results are consistent with previous studies (Silva et al. 2002) according to which the eutrophication conditions in Ria de Aveiro is unlikely to change as a result of the operation of the submarine outfall. From the management perspective, this methodology can support decision making in the implementation of treatment processes of the water discharged by the S. Jacinto outfall.

10.2.6 Seaweed Modeling

Seagrasses have a significant ecological importance in estuaries because they provide habitat for species which use them as a site for breeding, feeding and sheltering. Degradation of seagrass habitats negatively affects populations of species relevant for fishing.

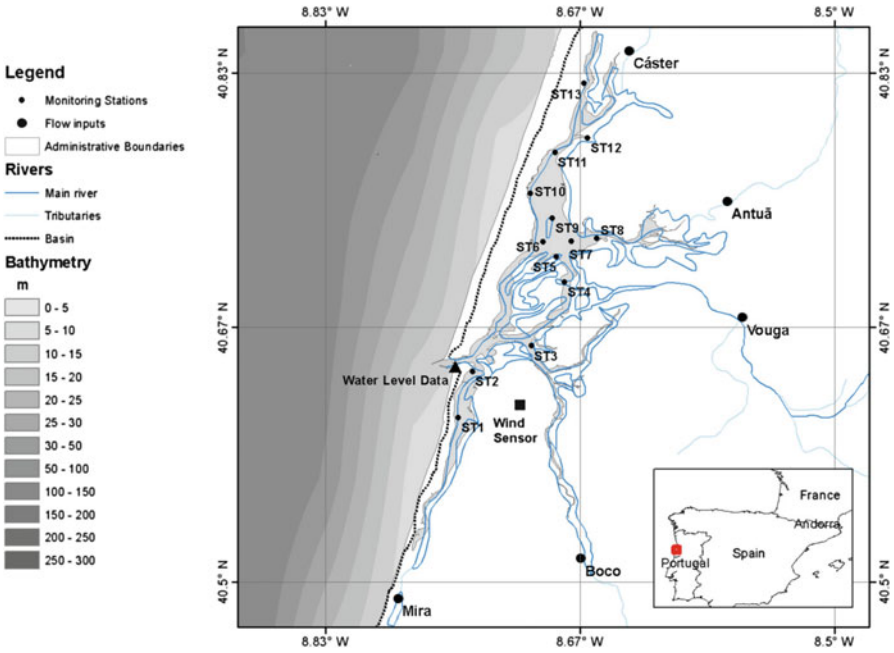

Fig. 10.21 Geographic location of Ria de Aveiro. Bathymetry of the study area, main rivers, flow inputs, wind sensor, and monitoring stations are indicated as well

In Portugal, seagrass habitat experienced a decline in the last 20 years (Cunha et al. 2013), causing biodiversity loss and degradation of coastal fisheries and water quality. *Zostera noltii* coverage in Ria Aveiro, Portugal, was about 8 km^2 in 1984, and it decreased down to 3 km^2 in 2004 (Silva et al. 2009; Cunha et al. 2013). The location of the Ria de Aveiro is described in Fig. 10.21. This decline in Ria Aveiro was attributed to a combination of factors such as dredging, deepening of channels, loss of fine sediments, siltation, nutrient washing, increasing tidal wave penetration, and increasing water currents. In Ria de Aveiro, the reduction of areas covered by seagrasses was followed by an increase of the areas of uncovered sediment, supporting the growth of sparse macroalgae populations only (Silva et al. 2009). Nutrient inputs from anthropogenic sources along Ria de Aveiro may trigger blooms of opportunistic macroalgae which could compete with other primary producers such as *Zostera noltii*.

A seagrass model was coupled to MOHID to assess the distribution of *Zostera noltii* in Ria de Aveiro. In the model, plant's growth depends on light, temperature, internal nutrient content, external nutrient availability, photoperiodicity, and space availability. Leaves and roots dynamics were expressed as:

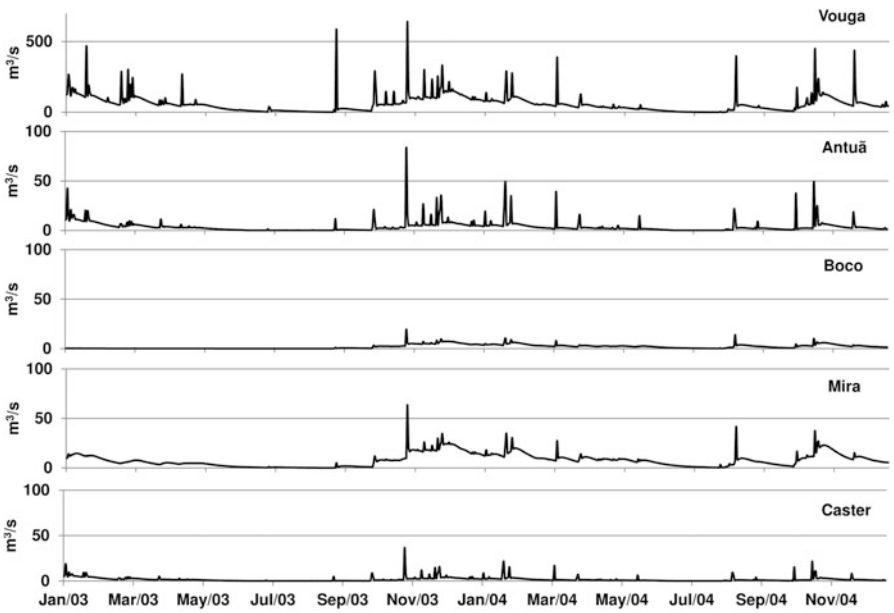

Fig. 10.22 Freshwater inflows at the main river canals, calculated by SWAT model applied to the Vouga catchment

$$\frac{dL}{dt} = (1 - tr)G \cdot L - m_l L \tag{10.10}$$

$$\frac{dR}{dt} = tr \cdot G \cdot L - m_r \cdot R \tag{10.11}$$

where L is the biomass of leaves (kg DW/m^2), R is the roots biomass (kg DW m^{-2}), m_r is the roots' decay rate (day^{-1}), and m_l is the leaves decay rate (day^{-1}). G is the growth rate (day^{-1}), and is a function of internal nutrient content. The full description of the seagrass model equations can be found in Ascione Kenov et al. (2013).

A 2-D hydrodynamic-biogeochemical model for Ria de Aveiro was used. The grid of the 2-D model had 87 × 81 cells and a variable resolution between 0.2 and 1 km (Fig. 10.21). The model was forced with average daily water inflows (Fig. 10.22) and nutrients coming from the main canals of Ria de Aveiro. These discharges were calculated by the Soil and Water Assessment Tool (SWAT), applied to the Vouga catchment.

At the open boundary, constant values were assumed for physical and biogeochemical properties. The model simulated hydrodynamics and water biogeochemistry, and provided fields of velocity, temperature, salinity, biogeochemical properties, and seagrass biomass, as output over time. The simulation time span

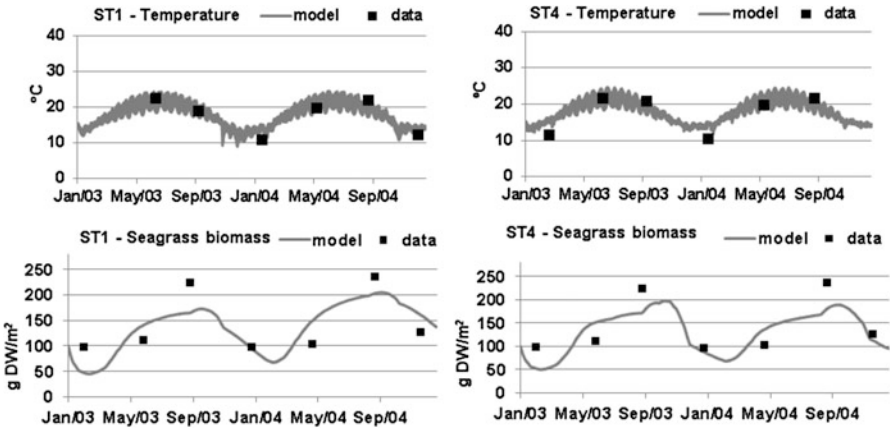

Fig. 10.23 Comparison between measured and simulated temperature and seagrass biomass (*Zostera noltii*)

was 2 years (between 01 January 2003 and 01 January 2005), with a time step varying between 10 and 15 s. Wind data used to force the hydrodynamic model were retrieved from the SNIRH database. Wind velocity and direction were measured by a Thies Clima/Young installed at a height of 2 m with respect to the ground level, at the Gafanha da Nazaré station (40.616°N, −8.706°E). The geographic location of the sensor is displayed in Fig. 10.21.

Temperature and *Zostera noltii* biomass data used to verify the model were collected by the University of Aveiro (Silva et al. 2009) in ten sampling points located in the intertidal areas of Ria de Aveiro with *Zostera noltii* beds, during the period between October 2002 and December 2004. A complete description of sampling methods and laboratory analysis used to retrieve *Zostera noltii* biomass can be found in Silva et al. (2009).

Results in Fig. 10.23 show comparison between data and model results for stations ST1 and ST4. The seagrass model outputs can be easily analyzed in the form of time series and maps, enabling easy calibration (Trancoso et al. 2005). The inclusion of the seagrass model in MOHID opened new possibilities to study interactions between primary producers (phytoplankton, macroalgae, and seagrasses) in response to natural and anthropogenic factors (nutrient inputs variations, temperature variations due to climate change, storms occurrence, among others). The flexibility of the model and its open source format enables to include new characteristics. For example, in the future the model may become more complex by adding a feedback effect by seagrasses over suspended sediment (seagrasses are capable to retain sediment), or over the bottom drag coefficient (seagrasses may alter the bed rugosity).

10.2.7 The Role of Complex Biogeochemical Algorithms in Estuarine Modeling

Estuaries are complex environments with their diverse biotic and abiotic conditions. Modeling approaches to simulate estuarine processes in water frequently rely on algorithms based on basic assumptions about the processes and constituents of marine systems. The advances which marine models underwent over the last decade (Vichi et al. 2003; e.g., Vichi et al. 2007a, b; Mateus et al. 2012a; Mateus 2012) are usually absent in estuarine model applications and leave out important components such as the microbial loop, phytoplankton composition, multiple nutrient limitation and the explicit modeling of the carbon cycle.

Despite the increase in the amount of model output in complex models, they provide additional knowledge and insights on the functioning of the system which are impossible to tackle with simpler algorithms. This section presents examples of the information provided by complex models. These examples are taken from published results of complex ecological models applied to the Tagus estuary, Portugal. The model is a biomass-based pelagic biogeochemical model (Mateus et al. 2012c) based on the ERSEM biochemical modeling philosophy (Baretta-Bekker et al. 1997; Baretta et al. 1995); it has 12 major components: producers, consumers, decomposers, organic matter (particulate, dissolved labile and semi-labile), nutrients (nitrate, ammonium, phosphate, silicate), biogenic silica and oxygen. The model has a decoupled nutrient and carbon dynamics with explicit parameterization of carbon, nitrogen, phosphorus, silica and oxygen cycles, and all living groups have variable stoichiometry and chlorophyll synthesis is accounted for in producers, allowing variable C:Chla ratios.

Complex ecological models can capture some of the complexity of estuarine system and provide reasonable estimates of the trends of the studied system. However, complex model generate a significant amount of results, and the calibration-validation effort can become a difficult task because just a few state-variables can be compared with field data. The results, even when not evaluated against data, and can still provide relevant information on the processes they address, helping to test hypotheses or raise additional relevant questions.

10.2.7.1 Nutrient Availability

The dynamics of nutrients depend on a number of physical, biological and chemical processes. Physical processes include mixing, flushing and sedimentation. Biological processes include fixation of dissolved and particulate nutrients, primarily by bacteria and phytoplankton, and release of inorganic nutrients through mineralization, mostly by bacterioplankton (decomposers).

Nutrients can be present in two major forms: inorganic (or mineral) and organic (both living and detrital). Nitrogen and phosphorus are the most significant nutrients, and their main species include dissolved (nitrate, nitrite, ammonium,

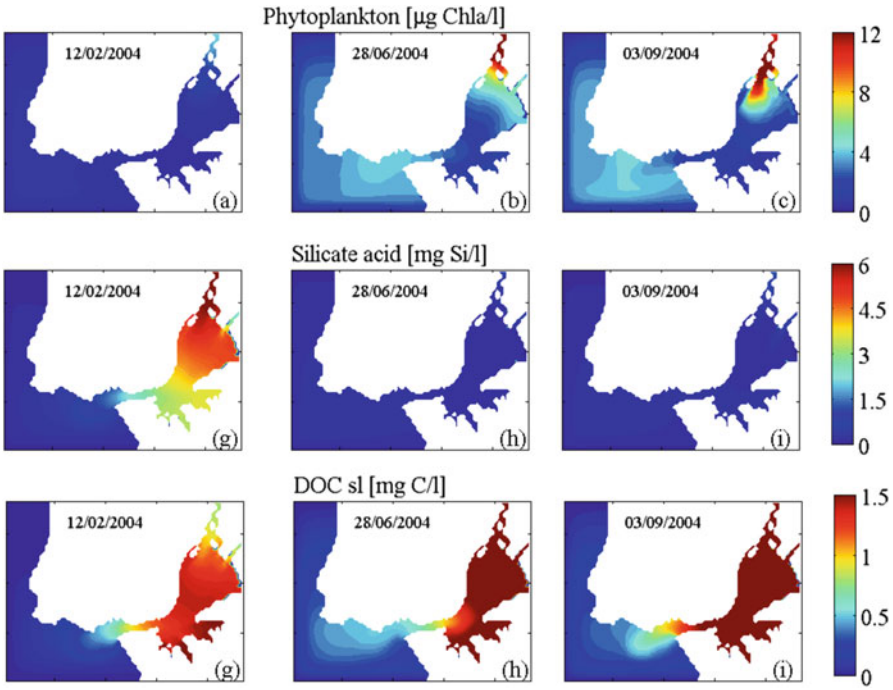

Fig. 10.24 Spatial maps for chlorophyll, silicate acid and semi-labile organic matter in a mesotidal estuary

organic N, phosphate, organic P) and particulate (organic N, organic P) components. Silica is also a fundamental nutrient in coastal systems because diatoms, a predominant phytoplankton group in estuaries and coastal systems, require silica in their structural composition. Complex model frequently address all of these properties, accounting for the explicit parameterization of several element cycles, thus tracing each nutrient and carbon source in the system. Figure 10.24 illustrates some of these results, with an example of spatial maps for chlorophyll, silicate acid and semi-labile organic matter in a mesotidal estuary.

There are no general rules to predict which nutrients limit estuarine primary producers, and when. Frequently nitrogen is the limiting nutrient, but even so, the limitation imposed by this nutrient may have significant temporal and spatial variations. Complex models are usually based on the assumption of variable internal nutrient composition, allowing to trace the evolution of C: Nut ratios in time for phytoplankton, and providing relevant clues on the influence of nutrient deficiency.

10.2.7.2 Light Conditions

Many estuaries are relatively shallow. In some systems this can provide optimal underwater light climate for primary production, but the high concentrations of suspended sediment greatly reduces the penetration of light through the water column. If the sediment is systematically suspended, then the consequent high turbidity and low light levels will reduce bloom conditions, regardless of nutrient levels. The result is that in many estuaries light is a key limiting factor for primary production (Cloern 2001), and there is a natural tolerance to eutrophication, i.e., a lack of a significant response to the nutrient loading in their inflowing rivers.

Phytoplankton responds to the variation in the light regime and nutrient availability across the temporal and spatial scales in estuaries. One of the most important physiological responses is the adjustment of chlorophyll content to maximize the use of available radiation. Phytoplankton will react to low light availability by increasing chlorophyll synthesis and this, in turn, will affect the C:Chla ratio of the cells. Models with this adjustment mechanisms (e.g., Mateus et al. 2012a) have proven useful for the understanding of how different ambient conditions influence the fluctuation of the C:Cha ratio. This is exemplified by model results in Fig. 10.25a, b, where the temporal and spatial C:Chla ratio of diatoms and autotrophic flagellates is shown to vary, as a response of ambient conditions (nutrient and light availability).

10.2.7.3 Relevant Ecological Groups

Most marine models rely on the assumption of a simple NPZD (nutrient-phytoplankton-zooplankton-detritus) chain, frequently addressing one group of phytoplankton and ruling out explicit parameterization of bacterioplankton. Complex models, on the other hand, usually have a functional approach for organisms, with more than one phytoplankton group and with bacterioplakton as a state-variable.

Regarding phytoplankton composition, estuaries show a significant diversity of species, but this variety can be addressed by considering two functional groups: diatoms (silica dependent) and autotrophic flagellates (silica independent). A simple approach with two phytoplankton groups provides significant insights on the nutrient limitation patterns inside estuaries, mostly related to the decrease in the concentration of some nutrients, such as phosphorus and silica, from the inner estuary to the estuary mouth. The fact that diatoms depend also on silica can explain in some cases the change in the phytoplankton composition, like the shift in diatom dominance from the inner estuarine areas to autotrophic flagellate dominance near the coast. Complex models can attempt to reproduce this shift, as in the example provide in Fig. 10.25c where diatom dominance decreases towards the estuary mouth, and silica-independent producers become dominant. These results may point to systematic shortage of dissolved silica in the lower estuarine areas, especially when flushing from the river is reduced.

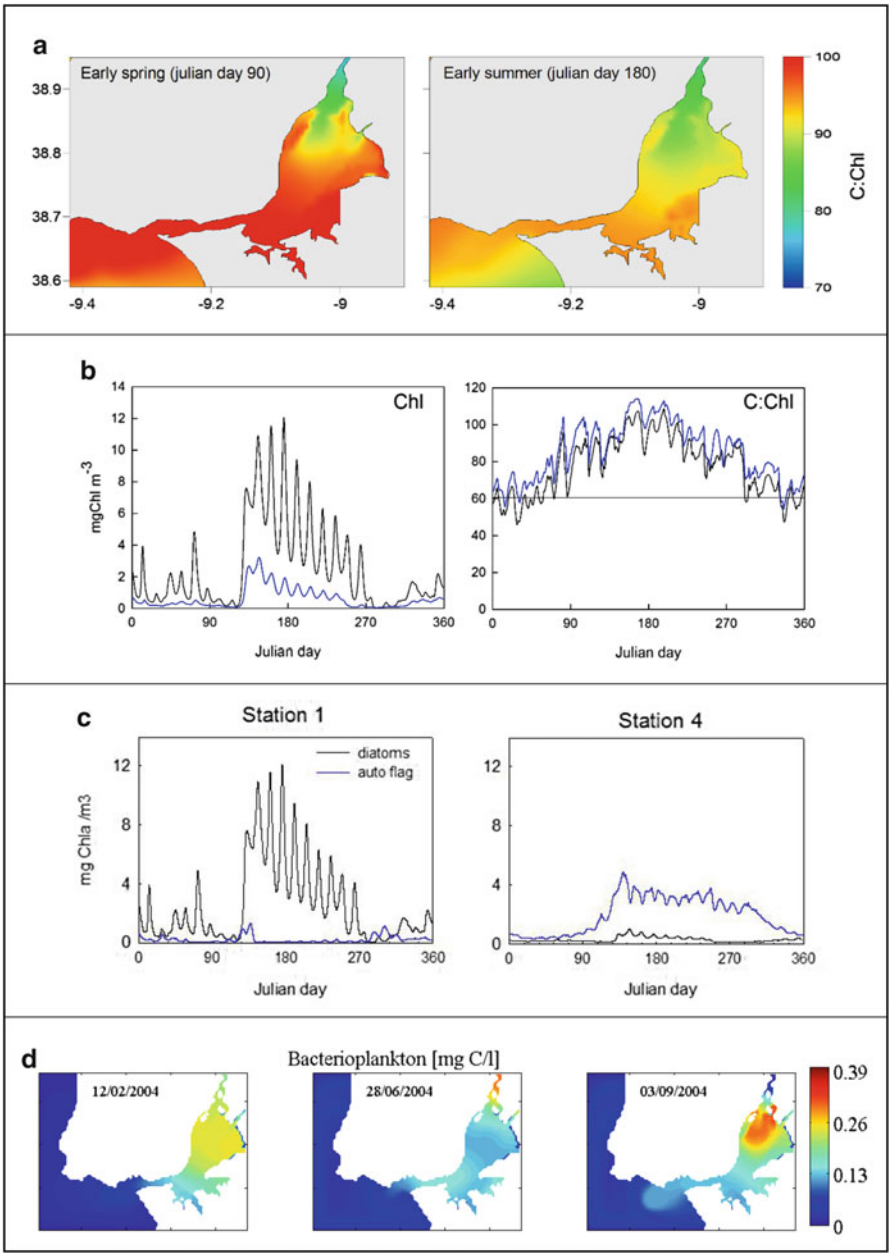

Fig. 10.25 Spatial patterns at different times of year obtained with a complex model that includes algorithms to address the bacterial loop

Bacterioplankton has a crucial role on the nutrient and carbon cycles in estuaries. Estuarine zones are usually dominated by allochtonous inputs of organic matter which promote the growth of heterotrophic organisms like bacteria, and for that reason estuarine waters are 1–3 orders of magnitude richer in bacterioplankton than the open ocean (Borsheim 2000). Since the availability of organic substrates for bacterioplankton growth varies significantly in estuaries, bacteria abundance will also vary, thus having a different impact on oxygen concentrations and nutrient release by mineralization of organic matter in different areas of the estuary. For their important role, bacterioplankton should be included in ecological models for estuaries, with all the complexity of the microbial loop and carbon-source substrates. Figure 10.25d shows significantly distinct spatial patterns at different times of year obtained with a complex model which includes algorithms to address the bacterial loop.

10.3 Conclusions

This chapter presented advanced modeling applications to address relevant water quality management questions related to estuarine water quality. Several case studies related to water quality assessment and management in Portuguese estuaries were presented. The described downscaling techniques enabled the integration of regional operational models with local scale models, improving open boundary conditions for estuarine models. The integration of regional and local scale models enabled the extension of operational forecasts to the local scale as well, and to the answering to common management questions, such as residence time of water. The presented modeling tools were used to complement the assessment of bathing water quality, and to answer NBWD statements. A new risk prediction methodology was proposed and applied to the Estoril coast to give timely predictions of fecal contamination of coastal waters. With the implementation of this methodology beach managers can predict the risk of contamination events and to prevent bathers from being exposed to pollution. The presented case studies show an effort to integrate different scales and to transfer information between hydrodynamic-ecological models, meteorological models, and watershed models, providing advancements to previous research carried out in this area (Dias et al. 2000; Trancoso et al. 2005; Lopes et al. 2009; Bierman et al. 2011; Mateus et al. 2012b). This approach can strongly improve the knowledge of the interconnections between land, ocean and atmosphere, moving forward the development of integrated models.

Acknowledgments Professor J.F. Da Silva of the Aveiro University for kindly providing monitoring data collected in Ria de Aveiro. Dr. Pedro Chambel, for kindly providing data of nutrients and freshwater inflows, calculated by using the SWAT model applied to the Vouga catchment. SANEST Project, S.A. (Saneamento Básico da Costa do Estoril) – Guia Submarine Outfall Monitoring Program. RECONNECT research project funded by Fundação para a Ciencia e

Tecnologia (FCT), under contract n. PTDC/MAR/64627/2006. LENVIS Project (FP7-ICT-2007/2/223925) financed by 7 FP7 of the European Commission. EASYCO Project, financed by the Atlantic Area Transnational Programme of the European Commission (EC), priority 2, through the European Regional Development Fund (ERDF), contract n. 2008-1/002. EMoSEM Project, contract n. SD/ER/11, financed under the network program ERANET SEAS-ERA "Towards Integrated Marine Research Strategy and Programmes".

References

Ali A, Lemckert CJ, Zhang H, Dunn RJK (2013) Sediment dynamics of a very shallow subtropical estuarine lake. J Coast Res. doi:10.2112/JCOASTRES-D-12-00255.1

Ascione Kenov I, Garcia AC, Neves R (2012) Residence time of water in the Mondego estuary (Portugal). Estuar Coast Shelf Sci 106:13–22. doi:10.1016/j.ecss.2012.04.008

Ascione Kenov I, Deus R, Alves CN, Neves R (2013) Modelling seagrass biomass and relative nutrient content. J Coast Res. doi:10.2112/JCOASTRES-D-13-00047.1

Baretta JW, Ebenhoh W, Ruardij P (1995) The European-regional-seas-ecosystem-model, a complex marine ecosystem model. Neth J Sea Res 33(3–4):233–246

Baretta-Bekker JG, Baretta JW, Ebenhoh W (1997) Microbial dynamics in the marine ecosystem model ERSEM II with decoupled carbon assimilation and nutrient uptake. J Sea Res 38(3–4):195–211

Bierman P, Lewis M, Ostendorf B, Tanner J (2011) A review of methods for analysing spatial and temporal patterns in coastal water quality. Ecol Indic 11(1):103–114. doi:10.1016/j.ecolind.2009.11.001

Borsheim KY (2000) Bacterial production rates and concentrations of organic carbon at the end of the growing season in the Greenland Sea. Aquat Microb Ecol 21(2):115–123

Braunschweig F, Martins F, Chambel P, Neves R (2003) A methodology to estimate renewal time scales in estuaries: the Tagus Estuary case. Ocean Dyn 53(3):137–145. doi:10.1007/s10236-003-0040-0

Bulleri F, Chapman MG (2010) The introduction of coastal infrastructure as a driver of change in marine environments. J Appl Ecol 47:26–35

Campuzano F, Nunes S, Malhadas MS, Neves R (2010) Modelling hydrodynamics and water quality of Madeira Island. GLOBEC Int Newsl 16(1):40–42

Campuzano F, Fernandes R, Leitão P, Viegas C, De Pablo H, Neves R (2012) Implementing local operational models based on an offline downscaling technique: the Tagus estuary case. In: 2.as Jornadas de Engenharia Hidrográfica, Lisbon, 20–22 June 2012, pp 105–108

Canteras JC, Juanes JA, Pérez L, Koev KN (1995) Modelling the coliforms inactivation rates in the Cantabrian Sea (Bay of Biscay) from in situ and laboratory determinations of t90. Water Sci Technol 32(2):37–44. doi:10.1016/0273-1223(95)00567-7

Chibole OK (2013) Modeling River Sosiani's water quality to assess human impact on water resources at the catchment scale. Ecohydrol Hydrobiol 13(4):241–245. doi:10.1016/j.ecohyd.2013.10.003

Choi KW, Lee JHW (2004) Numerical determination of flushing time for stratified water bodies. J Mar Syst 50(3–4):263–281. doi:10.1016/j.jmarsys.2004.04.005

Cloern JE (2001) Our evolving conceptual model of the coastal eutrophication problem. Mar Ecol Prog Ser 210:223–253

Cucco A, Umgiesser G (2006) Modeling the Venice Lagoon residence time. Ecol Model 193(1–2):34–51. doi:10.1016/j.ecolmodel.2005.07.043

Cunha AH, Assis JF, Serrão EA (2013) Seagrasses in Portugal: a most endangered marine habitat. Aquat Bot 104:193–203

Deus R, Brito D, Ascione KI, Lima M, Costa V, Medeiros A, Neves R, Alves CN (2013) Three-dimensional model for analysis of spatial and temporal patterns of phytoplankton in Tucuruí reservoir, Pará, Brazil. Ecol Model 253:28–43

Dias JM, Lopes JF, Dekeyser I (2000) Tidal propagation in Ria de Aveiro Lagoon, Portugal. Phys Chem Earth B 25(4):369–374

Fernandes R (2005) Modelação operacional no estuário do Tejo. Instituto Superior Técnico, Technical university of Lisbon, Lisbon

Fernandes L, Saraiva S, Leitão PC, Pina P, Santos A, Braunschweig F, Neves R (2006) Mabene deliverable D4.3d-code and description of the benthic biogeochemistry module-managing benthic ecosystems in relation to physical forcing and environmental constraints. MaBenE-Managing benthic ecosystems in relation to physical forcing and environmental constraints

Grell G, Dudhia J, Stauffer D (1994) A description of the fifth-generation Penn State/NCAR Mesoscale Model (MM5)

IST, SANEST (2004) Bacteria mortality tests considering different environmental parameters

Lai YC, Tu YT, Yang CP, Surampalli RY, Kao CM (2013) Development of a water quality modeling system for river pollution index and suspended solid loading evaluation. J Hydrol 478(0):89–101. doi:10.1016/j.jhydrol.2012.11.050

Leitão P, Coelho H, Santos A, Neves R (2005) Modelling the main features of the Algarve coastal circulation during July 2004: a downscaling approach. J Atmos Ocean Sci 10(4):421–462. doi:10.1080/17417530601127704

Leitão P, Galvão P, Aires E, Almeida L, Viegas C (2012) Faecal contamination modelling in coastal waters using a web service approach. Environ Eng Manag J 11(5):899–906

Lopes JF, Cardoso AC, Moita MT, Rocha AC, Ferreira JA (2009) Modelling the temperature and the phytoplankton distributions at the Aveiro near coastal zone, Portugal. Ecol Model 220 (7):940–961. doi:10.1016/j.ecolmodel.2008.11.024

Mateus M (2012) A process-oriented model of pelagic biogeochemistry for marine systems. Part I: model description. J Mar Syst 94:S78–S89. doi:10.1016/j.jmarsys.2011.11.008

Mateus M, Leitão PC, de Pablo H, Neves R (2012a) Is it relevant to explicitly parameterize chlorophyll synthesis in marine ecological models? J Mar Syst 94:S23–S33. doi:10.1016/j.jmarsys.2011.11.007

Mateus M, Riflet G, Chambel P, Fernandes L, Fernandes R, Juliano M, Campuzano F, de Pablo H, Neves R (2012b) An operational model for the West Iberian coast: products and services. Ocean Sci 8(4):713–732. doi:10.5194/os-8-713-2012

Mateus M, Vaz N, Neves R (2012c) A process-oriented model of pelagic biogeochemistry for marine systems. Part II: application to a mesotidal estuary. J Mar Syst 94(Supplement):S90–S101. doi:10.1016/j.jmarsys.2011.11.009

Miranda R, Braunschweig F, Leitâo P, Martins F, Santos A (2000) MOHID2000 – a coastal integrated object oriented model. In: Hydraulic engineering software VIII. WIT Press

Neves R (2013) The MOHID concept. In: Mateus M, Neves R (eds) Ocean modelling in coastal management. IST Press, Lisbon, pp 1–11

Neves R, Silva A (1991) An extension of the Boussinesq equations to deep water. A case study. Paper presented at the computer modelling in ocean engineering, Barcelona

Neves R, Viegas C, Fernandes R, Nunes S, Pina P, Carvalho C, Granger C (2010) Ferramentas matemáticas de suporte à definição de perfis de água balnear: 2 casos de estudo, vol 30, 90th edn, Recursos Hídricos. Associação Portuguesa dos Recursos Hídricos, Lisbon

Pando S, Juliano MF, García R, de Jesus Mendes PA, Thomsen L (2013) Application of a lagrangian transport model to organo-mineral aggregates within the Nazaré canyon. Biogeosciences 10(6):4103–4115. doi:10.5194/bg-10-4103-2013

Pinto L, Campuzano F, Fernandes R, Fernandes L, Neves R (2012) An operational model for the Portuguese coast. In: 2.as Jornadas de Engenharia Hidrográfica, Lisbon, 20–22 June 2012, pp 85–88

Silva JF, Duck RW, Anderson JM, McManus J, Monk JGC (2001) Airborne observations of frontal systems in the inlet channel of the Ria de Aveiro, Portugal. Phys Chem Earth B Hydrol Oceans Atmos 26(9):713–719. doi:10.1016/S1464-1909(01)00075-2

Silva J, Duck RW, Hopkins TS, Rodrigues M (2002) Evaluation of the nutrient inputs to a coastal lagoon: the case of the Ria de Aveiro, Portugal. Hydrobiologia 475–476(1):379–385. doi:10.1023/A:1020347610968

Silva JF, Duck RW, Catarino JB (2009) Nutrient retention in the sediments and the submerged aquatic vegetation of the coastal lagoon of the Ria de Aveiro, Portugal. J Sea Res 62:276–285

Sohma A, Sekiguchi Y, Kuwae T, Nakamura Y (2008) A benthic-pelagic coupled ecosystem model to estimate the hypoxic estuary including tidal flat-model description and validation of seasonal/daily dynamics. Ecol Model 215:10–39

Trancoso AR, Saraiva S, Fernandes L, Pina P, Leitão PC, Neves R (2005) Modelling macroalgae using a 3D hydrodynamic-ecological model in a shallow, temperate estuary. Ecol Model 187:232–246

Vichi M, Oddo P, Zavatarelli M, Coluccelli A, Coppini G, Celio M, Umani SF, Pinardi N (2003) Calibration and validation of a one-dimensional complex marine biogeochemical flux model in different areas of the northern Adriatic shelf. Ann Geophys Germany 21(1):413–436

Vichi M, Masina S, Navarra A (2007a) A generalized model of pelagic biogeochemistry for the global ocean ecosystem. Part II: numerical simulations. J Mar Syst 64(1–4):110–134

Vichi M, Pinardi N, Masina S (2007b) A generalized model of pelagic biogeochemistry for the global ocean ecosystem. Part I: theory. J Mar Syst 64(1–4):89–109

Viegas C, Nunes S, Fernandes R, Neves R (2009) Streams contribution on bathing water quality after rainfall events in Costa do Estoril – a tool to implement an alert system for bathing water quality. J Coast Res Proc 10th Int Coast Symp ICS 2009 II(Special Issue No. 56):1691–1695

Viegas C, Neves R, Fernandes R, Mateus M (2012) Modelling tools to support an early alert system for bathing water quality. Environ Eng Manag J 11(5)

Viero DP, D'Alpaos A, Carniello L, Defina A (2013) Mathematical modeling of flooding due to river bank failure. Adv Water Resour 59(0):82–94. doi:10.1016/j.advwatres.2013.05.011